NUMERICAL ANALYSIS OF BLAST PRESSURE PARAMETERS ON THE VEHICLE WITH AND WITHOUT WALL AS A BARRIER

NOR FADLIHA BINTI AZIZ

B. ENG (HONS.) CIVIL ENGINEERING

UNIVERSITI MALAYSIA PAHANG

UNIVERSITI MALAYSIA PAHANG

DECLARATION OF THESIS AND COPYRIGHT

Author's Full Name   : NOR FADLIHA BINTI AZIZ

Date of Birth   : 12 OCTOBER 1996

Title   : NUMERICAL ANALYSIS OF BLAST PRESSURE PARAMETERS ON THE VEHICLE WITH AND WITHOUT WALL AS A BARRIER

Academic Session   : 2018/2019

I declare that this thesis is classified as:

☐   CONFIDENTIAL   (Contains confidential information under the Official Secret Act 1997)*

☐   RESTRICTED   (Contains restricted information as specified by the organization where research was done)*

☑   OPEN ACCESS   I agree that my thesis to be published as online open access (Full Text)

I acknowledge that Universiti Malaysia Pahang reserves the following rights:

1. The Thesis is the Property of Universiti Malaysia Pahang
2. The Library of Universiti Malaysia Pahang has the right to make copies of the thesis for the purpose of research only.
3. The Library has the right to make copies of the thesis for academic exchange.

Certified by:

_____   _____
(Student's Signature)   (Supervisor's Signature)

Nor Fadliha Binti Aziz   Dr. Mazlan Bin Abu Seman

New IC: 961012115554   Name of Supervisor

Date: 17 June 2019   Date: 17 June 2019

NOTE : * If the thesis is CONFIDENTIAL or RESTRICTED, please attach a thesis declaration letter.

THESIS DECLARATION LETTER (OPTIONAL)

Librarian,
Perpustakaan Universiti Malaysia Pahang,
Universiti Malaysia Pahang,
Lebuhraya Tun Razak,
26300, Gambang, Kuantan.

Dear Sir,

CLASSIFICATION OF THESIS AS RESTRICTED

Please be informed that the following thesis is classified as RESTRICTED for a period of three (3) years from the date of this letter. The reasons for this classification are as listed below.

Author's Name
Thesis Title

Reasons   (i)

(ii)

(iii)

Thank you.

Yours faithfully,

_____
(Supervisor's Signature)

Date:

Stamp:

Note: This letter should be written by the supervisor, addressed to the Librarian, *Perpustakaan Universiti Malaysia Pahang* with its copy attached to the thesis.

STUDENT'S DECLARATION

I hereby declare that the work in this thesis is based on my original work except for quotations and citations which have been duly acknowledged. I also declare that it has not been previously or concurrently submitted for any other degree at Universiti Malaysia Pahang or any other institutions.

_____

(Student's Signature)

Full Name   : NOR FADLIHA BINTI AZIZ

ID Number   : AA15110

Date   : JUNE 2019

NUMERICAL ANALYSIS OF BLAST PRESSURE PARAMETERS ON THE VEHICLE WITH AND WITHOUT WALL AS A BARRIER

NOR FADLIHA BINTI AZIZ

Thesis submitted in fulfillment of the requirements
for the award of the
B. Eng (Hons.) Civil Engineering

Faculty of Civil Engineering and Earth Resources

UNIVERSITI MALAYSIA PAHANG

JUNE 2019

ACKNOWLEDGEMENTS

ABSTRAK

Perobohan struktur atau bangunan lama dengan menggunakan bahan letupan adalah salah satu kaedah yang digunakan dalam kerja-kerja pembinaan dan pembangunan di lokasi yang sedia ada. Malangnya, kaedah ini juga diguna pakai oleh pihak pengganas untuk mendapat perhatian pihak berkuasa tempatan atau antarabangsa. Serangan pengganas seperti ini rata-ratanya meragut nyawa apabila berlaku di tempat di mana pihak berkuasa tidak menjangka berlakunya tragedy seperti ini contohnya di kawasan kediaman termasuklah di dalam kenderaan. Oleh itu, apabila kenderaan terdedah kepada letupan ini, ia boleh memberi impak negatif terhadap struktur kereta itu dengan itu juga boleh mempengaruhi orang-orang di dalamnya. Ini kerana kebanyakan kenderaan tidak direka untuk menahan beban dinamik seperti peluru dan beban letupan, dan ia menawarkan hampir tidak ada perlindungan kepada penghuni di dalamnya kecuali kepada kenderaan-kenderaan itu untuk kegunaan khas seperti pegawai kerajaan dan pegawai kerajaan yang lebih tinggi. Oleh itu dalam kajian ini, parameter tekanan letupan dari letupan 13.61 kg (30 lbs.) TNT (trinitrotoluene) akan dinilai secara berangka. Untuk mencapai matlamat ini, ANSYS AUTODYN akan digunakan untuk mensimulasikan tekanan letupan di kawasan sekitarnya. Simulasi berangka yang pada mulanya dijalankan dalam letupan udara bebas 3D 1000 mm x 1000 mm x 5500 mm udara dan diikuti dengan pertimbangan dua lagi kes yang berbeza dengan meningkatkan domain udara 1219 mm x 3000 mm x 1112 mm jumlah udara. Susunan grid I, J, K (18, 22, 72) dipertimbangkan dalam kedua-dua kes yang tanpa sebarang halangan dinding dan dengan halangan tembok pada penyebaran gelombang letupan. Sebelum menjalankan sebarang simulasi, letupan awal bahan letupan dimodelkan. Pengesahan 30 lbs. TNT tolok yang terletak pada 5486 mm (18 kaki) dari berat caj akan disahkan dengan ujian letupan sebenar dalam penulisan sebelumnya oleh Yan et. al, (2011). Setelah pengesahan ini, bilah letupan yang sama telah diperbaiki dan digunakan untuk kes 2 dan kes 3; tanpa dan dengan dinding penghalang. Kemudian, hasil berangka diperolehi di kedudukan yang berbeza dari tolok dalam kes 2 dan case 3 dibentangkan dan dibandingkan. Keputusan menunjukkan bahawa tekanan tinggi untuk tolok 1 terletak pada jarak 1219 mm di hadapan berat cas untuk kes 3 adalah lebih tinggi berbanding dengan kes 2. Dibuktikan bahawa apabila gelombang menemui permukaan, ia dapat dilihat dan diperbesarkan tekanan . Selain itu, untuk tolok 2 terletak pada jarak 1369 mm dari pusat letupan di mana lokasi untuk kes 3; dengan dinding sebagai penghalang, tolok ini terletak betul-betul di belakang dinding. Ia menunjukkan bahawa tekanan untuk tolok ini dalam kes 3 adalah lebih rendah daripada dalam kes 2. Ini kerana apabila tangkapan dari gelombang letupan memberi kesan kepada dinding penghalang, ia akan meresap di sekitar dinding penghalang. Akibatnya, gelombang berkurang untuk beberapa jarak di belakang dinding. Selain itu, kesan tekanan letupan pada manusia di dalam kenderaan melebihi 250 kPa untuk kes 2 dan 220 kPa untuk kes 3, ini menyebabkan orang itu diambang kematian. Bagi kes 2 dan kes 3, kesan tekanan letupan ke atas manusia di luar kenderaan yang terdedah kepada tekanan tinggi yang lebih tinggi berbanding empat tolok lain kira-kira 540 kPa dan 510 kPa masing-masing. Oleh itu, orang di lokasi ini mungkin mengalami 100% kematian. Di samping itu, berdasarkan perbandingan antara dua kes yang berlaku untuk kes 2 dan kes 3, dapat disimpulkan bahawa tekanan tinggi untuk kes 3 lebih rendah daripada tekanan tinggi pada kes 2. Oleh itu, keputusan keseluruhan menunjukkan bahawa tekanan letupan dikurangkan apabila terdapat tembok penghalang berhampiran peristiwa letupan berbanding ketika tidak ada dinding pada peristiwa letupan.

ABSTRACT

Demolition of old structure or building by using explosive is one of the methods are used in construction and development works at an existing location. Unfortunately, this method also preferred by terrorist to gain attention from the local or international authorities. This kind of terrorist attack is lethal when occurred at the place where the authorities not expected to occur for example nearby the residential area including those in the vehicle. So when vehicles are exposed to this explosion, it could have a negative impact on the car's structure thus can also affect the people inside. This is because most of the vehicles are not designed to withstand the dynamic load such as bullet and blast load, and it does offer almost no protection to the occupants inside except to those vehicles for special purpose usage such as for royal and higher ranking government officer. Hence in this study, the blast pressure parameter from the explosion of 13.61 kg (30 lbs.) Trinitrotoluene (TNT) will be evaluated numerically. To achieve this objective, ANSYS AUTODYN will be used to simulate the blast pressure on the surrounding area. The numerical simulation initially conducted in 3D free air explosion of 1000 mm x 1000 mm x 5500 mm volume of air and followed by the consideration of another two different cases by increasing in air domain of 1219 mm x 3000 mm x 1112 mm volume of air. The grid arrangement of I, J, K (18, 22, 72) is considered in both cases which are without any obstruction of the wall and with obstruction of the wall on the blast wave propagation. Before running any simulation, the initial detonation of the explosive is modeled. The validation of 30 lbs. TNT of the gauge located at 5486 mm (18 ft.) from the charge weight will be verified with the actual blast test in previous literature by Yan et. al, (2011). After this verification, the same blast wedge was remapped and used for case 2 and case 3; without and with barrier wall respectively. Then, the numerical result obtained at different position of gauges in case 2 and case 3 is presented and compared. The results show that the peak overpressure for gauge 1 located at 1219 mm away in front of the charge weight for case 3 is instantaneously higher compared to case 2. It is proved that when the wave encounters a surface, it is reflected and magnified the overpressure. Besides that, for gauge 2 located at 1369 mm away from the explosive center where the location for case 3; with wall as a barrier, this gauge is located exactly behind the wall. It shows that overpressure for this gauge in case 3 is lower than in case 2. This is because when a charge from the blast wave impact the barrier wall, it will diffract around the barrier wall. As a result, the wave is lessened for some distance behind the wall. Moreover, the effect of the blast pressure on human inside the vehicle to an overpressure of 250 kPa for case 2 and 220 kPa for case 3, the person may result in threshold of fatalities. For case 2 and case 3, the effect of the blast pressure on human outside the vehicle which it exposed to the highest peak overpressure than the other four gauges about 540 kPa and 510 kPa respectively. So, the person at this location likely to experience 100 % of fatalities. In addition, based on the comparison between two cases which are for case 2 and case 3, it can be concluded that the peak overpressure for case 3 is lower than peak overpressure in case 2. Therefore, for overall results show that the blast pressure reduced when there is barrier wall nearby the blast event compared when there is no wall at blast event.

TABLE OF CONTENT

LIST OF TABLES

LIST OF FIGURES

LIST OF SYMBOLS

kPa	Kilopascal
Lbs	Pounds
Kg	Kilogram
M	Meter
mm	Millimetre
Psi	Pound per square inch
Ft	Feet
MPa	Mega Pascal
Gpa	Giga Pascal

LIST OF ABBREVIATIONS

TNT	Trinitrotoluene
RC	Reinforced Concrete
^{O}C	Degree Celcius
FE	Finite Element
CFD	Finite Volume
SPH	Mesh Free Particle
ALE	Arbitrary lagrange euler
2D	2 Dimension
3D	3 Dimension
RHT	Reidel, Hiermayer and Thoma
JC	Johnson and Cook
JWL	Jones-Wilkins-Lee
EOS	Expression of state

CHAPTER 1

INTRODUCTION

1.1   Background Study

An explosion is a sudden release of energy which it interactions with an object start with rapid chemical reactions accompanied by explosive detonation. As the shock wave propagates in the medium of the explosion product, it affects the object. With the capability to release energy, an explosion technique by using different explosive such as physical, nuclear and chemical explosions are widely used for the demolition of existing structure in development and construction works. Unfortunately, the explosion method also prefers by the terrorists to gain the attention from the authority to fulfil their request. From the record, most of the terrorist attack occurred at main attraction places with dense of civilian around. For example, the attack on World Trade Centre towers and the Pentagon, thousands of them were killed and injured on September 11, 2001 (Kontodimos, 2017). Therefore, it come an interest to protect or minimize the blast impact on the surrounding area by designing reliable building or infrastructure which is able to protect the people who lives and work nearby. Thus, blast barrier walls can be used to mitigate explosive damage to target structures such as to the civilian vehicle that would otherwise be adversely affected by an explosive charge detonation blast. In this case, the barrier walls serve two purposes which are they ensure that an explosive charge is set away from a protected object at a standoff distance and diffract blast waves to a point to mitigate the full force of the protected object's blast pressures especially to the nearby vehicle.

1.2   Problem Statement

An engineer is responsible to design structure to withstand in any possible types of different load. Although it is possible for the engineer to design the structural that able to fully withstand the blast loads but it is expensive and not economical for the civilian structure. For example, when the blast occurs at residential area, the blast pressure will cause tremendous impact to the surrounding area especially to the vehicle park nearby if only the wire fence were provided. However, if construction of reinforced concrete as a barrier wall at the boundary or residential perimeter, wall barrier can effectively reduce the blast impact and one of the effective ways of ensuring the safety of nearby civilians. For instance, the use of perimeter protection or barrier walls like fences and guard is to reduce sound pollution. But by constructing this barrier, it can have a big impact on the surrounding people as it gives the limitation and mitigates the explosion from propagating too much pressure on the object as on the vehicles behind the wall. In addition, the existing barrier wall can extend the effect of the nearby parking vehicle on the pressure reduction area.

Most of the civilian vehicles are not designed to withstand the dynamic load such as bullet, blast load and it offer almost no protection to the occupants inside except to those vehicles for special purpose usage such as for royal and higher ranking government officer. If the explosions occur at the civilian vehicle, it will propagate it pressure in the higher temperature. So when the cars are exposed to that explosion, it might give the bad impact to the structural of the car. In the worst thing, this blast also can effect to the people inside.

1.3   Objectives of the Research

The research is to consider several principal aims which is important to achieve certain expected results. To achieve the aim of this study, the following objectives have been set as:

1. To investigate the blast overpressure parameters of 13.61 kg (30 lbs.) trinitrotoluene (TNT)

2. To study the blast pressure profile on vehicle with and without wall as a barrier.

3. To observe the possible effect of blast pressure on human inside and outside the vehicle.

1.4 Scope of the Research

The scope of this research is only to focus about the blast pressure to the vehicle with or without the Reinforced concrete (RC) wall regarding to the 30-lbs TNT blast load. The research will include all this scope in order to achieve the objectives and to make sure this study is in the right flow; this are the following scopes:

1. ANSYS AUTODYN will be used to simulate the blast pressure in different cases.
2. In the numerical analysis simulation, there are three possible cases will be considered which are; blast in open space, blast without wall as a barrier and blast with wall as a barrier.
3. In the first part, the numerical modelling of RC wall subjected to 13.61 kg (30 lbs.) TNT in AUTODYN. The simulation result will be verified by the blast test on the RC wall available in the previous literature by Yan et al., (2011).
4. After that, the same blast wedge was remapped and used for the next cases which are for the case with and without RC wall as barrier.
5. The possible impact on human inside and outside the vehicle due to blast pressure.
6. The results will be compared and discussed.

1.5 Significant of the Research

Study of blast pressure behaviour and effect is important, especially to the vehicle with and without the barrier wall. Since next threat by the terrorist activities cannot be predicted and determined, by conducting this study case it may help to reduce the blast effect on the government buildings, embassy building and public places such as airport. This is because of the blast loads; exceptional case which is the man-made disasters need to be given more attention just like the cases of earthquake and wind loads. In addition, to achieve the continuity function of that structure after the explosion, the architectural and structural factors must put it together with the optimum way in building plan design.

Besides that, the validation of the experimental data using numerical modelling of 13.61 kg (30 lbs.) TNT for the gauge at 18 ft. from the charge weight versus the experimental part of the blast test by previous researcher Yan et al., (2011). It is proved that the further parametric study can be carried out without additional cost. Therefore, the numerical study is possible to carry out since there is limited access for civilians to conduct the actual blast test which need the military provision first. This reduces the cost for constructing the RC wall, prepare the explosive material and area for testing.

The other reason in doing this research is to hinder and minimize the casualty and fatality to innocent civilians within the surrounding parameter especially nearby to the cars from causing in additional injuries and deaths. For example, they may be affected by the car debris caused by the explosion. Additionally, the most important things are the human safety should be provided responsibility. When the bomb started to explode, the area surrounding will become overpressure. It will result in high air particle that travels much faster than the speed of sound which only for a few milliseconds. So when it reached to a person, the person will feel the force of that blast and finally feel the initial impact of the shockwave. In result, it will give the impact damage to the body.

1.6   Outline of the Thesis

Chapter 1 presents a general introduction of overall study case which is about blast pressure parameter on the vehicle with and without reinforced concrete wall as a barrier and a discussion of the problem, the objectives, the scope of the research and significant of research.

Chapter 2 will be further explained on overall research details by considering the case study of investigation on 13.61 kg (30 lbs.) TNT blast parameter with and without wall based on references such as research articles, books, internet, and journals. For the current research, AUTODYN simulation package was used.

Chapter 3 then deals with the methodology of research. This chapter will explain more about how this research project is being conducted. In essence, this chapter also consists of the research project's flow procedures.

Chapter 4 is about the simulation analysis result and result discussions. ANSYS AUTODYN is used to model and analyse the result in simulation, as well as to identify the blast pressure in the different location of the gauges. The numerical result obtained at different position of gauges are presented and compared.

Chapter 5 presents the experimental results and numerical validation of the blast pressure with or without RC wall as barrier to the vehicles. This chapter also includes recommendations from the overall conclusion.

CHAPTER 2

LITERATURE REVIEW

2.1   Introduction

The purpose of this literature review was to study the theoretical background about the numerical analysis of the blast pressure on the vehicle with and without the wall as a barrier through journals, books, internet and articles. The study was related to the aim and objectives of this study. All we all know, the explosive devices are widely used for the demolition purposes in development and construction work. Unfortunately, by using this method, many buildings have been attacked by the terrorist activities. For example, important structures such as embassies, airport and government buildings become one of the potential targets to the terrorist. So, when the explosion occurs, it emits the blast wave in high pressure which can destroy the vehicles nearby and people surrounding. Figure 2.1 below show the examples of the terrorist attacks on the civilian vehicles. Thus, for these specific study, the numerical simulations are used to estimate the blast pressure at certain points surrounding the vehicle and the overview of the blast overpressure.

Figure 2.1 The blast effect on the car structure.

2.2   Blast

A blast or explosion is a sudden release of energy in a risky way by rapid chemical reactions. The released energy is commonly in an explosion of TNT (symmetrical 2,4,6-trinitrotoluene). It usually the generation of high temperatures and it takes the form of light, sound, heat and shock wave. Draganić and Sigmund (2012) stated that only about one third of the total chemical energy is released by detonation and the remaining two thirds are released slowly in the blasts as the explosive products mix with surrounding air and burn. The large pressure difference is being created through the explosion and it is known as a shock wave. The shock wave is an air pressure in the compressed form that moving outward radially from the source at supersonic velocities and it moves spherically away from the explosion point. The shock wave impinges the object when it propagates in the explosion product medium. The object responds to the impingement of the initial blast wave and the interaction leads to a series of complex, multi-physics phenomena (Yang et al., 2013).

Besides that, there are three categories of explosions which are (1) physical; (2) nuclear and (3) chemical explosions. The chemical explosions are one of the commonly used for terrorist attacks to manufacture the bomb. The main sources of energy in the chemical explosions are the rapid corrosion of fuel elements; carbon and hydrogen atoms. According to the Lippincott (2015), an explosive substance is a solid or liquid substance which is in itself capable by chemical reaction of producing gas at such a temperature and pressure and at such a speed as to cause damage to the surroundings. In this context, the effect of explosion can increase the air pressure and it followed by the release of the heat and light in the fast situation. Ramasamy et al., (2013) highlighted that as the detonation products expand, forcing out the volume it occupies, a layer of compressed air (blast wave) forms in front of this gas volume. So, the blast pressure and impulse will produce by an explosion.

Moreover, detonation of the explosive material occurs from the instantaneous conversion of solid or liquid into gas. According to Wolf et al. (2009), the gas will rapidly expands outwards from the point of detonation and displaces the surrounding medium, usually air or water. Thus, it can cause the raising of pressure that will create the blast wave dissipated over distance and time. When the blast wave travels through the air, the pressure wave dissipates in inverse proportion to the third power of the

distance from the detonation point (Ramasamy et al., 2013). In result, the immediate propagation of the blast wave will propel the object such as vehicles explode and thus causing injury of the nearby civilians.

However, when the charge is on the ground, it will propagate hemispherical through the air. Furthermore, the shockwave will become weaker if it travels in the long distance from the point of explosion. So, the negative wave is formed after the initial pressure wave travels through an area which it creates a vacuum state as shown in figure 2.2. The figure defined that the shock waves are characterized by a compression phase (positive phase) with a very high peak pressure and a following undertow phase (negative phase) (Alexander et al., 2013). In the compression phase, the pressure starts with a shock front that shows a strong increase in the pressure from the ambient pressure (p0) to the peak pressure within a timescale of nanoseconds (Alexander et al., 2013).
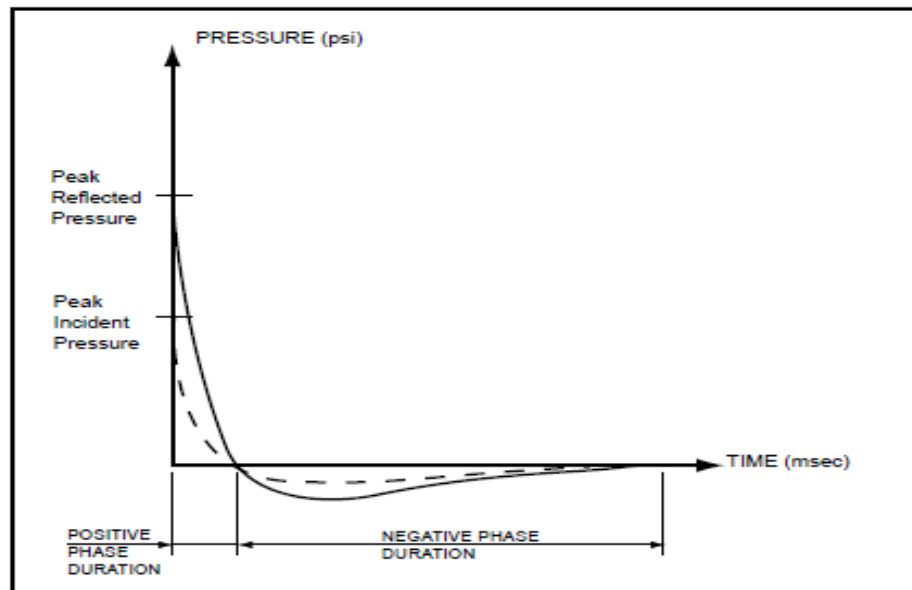
Figure 2.2 Simplified sketch of the blast pressure versus time

During the negative phase of the blast wave, usually it can cause less direct damage to the material surrounding it for example the car's window gets cracked or broken. Generally, it is quite a small contrast with the positive peak pressures which all the direct destruction can occur in the positive phase which caused by both dynamic

pressure and overpressure. Thus, it will significantly show the associated destructive effects to the car.

2.2.1   Blast Loading Classification

Blast loads can be categorized into two major groups such are unconfined and confined explosions based on the explosive charge as shown in table 2.1. Besides that, it can be sub-divided into some categories for each major based on the blast loading that produced to the structure or acting on the structure.

Table 2.1 Blast Load Categories

Charge Confinement	Categories
Unconfined	The explosion in the free air
	The explosion in the air
	The explosion near the ground
Confined	Full ventilation
	Partially confined
	Fully confined

Source: Draganić and Sigmund (2012).

The free air blast pressure or open-air explosion is occurring between the explosive charge and the structure which it spreads it wave without any amplification of the initial shock wave. According to Draganić and Sigmund (2012), these explosions are situated at a given distance and height away from the structure and there is a wave increase due to the reflection of the ground before it contact the structure and the height limitations of these explosions are two to three times of the height of a one-storey or two-storey structure. Besides that, Mirgal et al. (2014) stated the unconfined explosions can occur as an air-burst or a surface burst. The air burst environment or the explosion in the air is produced by explosions that occur above the ground surface and at a distance away from the building structure so that the initial shock wave, propagating away from the explosion, impinges on the ground surface prior to arrival at the structure (Remennikov, 2007). Furthermore, the explosion is considered as surface burst when the charge is located near or on the ground. The initial wave of the explosion is

reflected and reinforced by the ground surface to produce a reflected wave (Olarewaju et al., 2010).

For confined explosion, the peak pressure associated with the initial wave is very high when the explosion occurs in the structure because the refraction within the structure have been enhanced. Furthermore, depending on the degree of confinement, high temperatures and the accumulation of gaseous products of chemical reactions in the blast would produce more pressure and increase the load duration within the structure (Draganić and Sigmund, 2012). So, due to the increase combined effects of this pressure, it can lead to the damage to the car.

2.2.2 Propagation of the Blast Wave

Normally, there are three types of reflection that give an effect or impact in a negative way on a surface such as normal reflection, oblique reflection and Mach stem reflection. The simplest type is the normal reflection that occurs when the incident angle is zero degree, 0°. The reflected pressure for normal reflection is larger than that for oblique and Mach stem reflections, which occur when there is an incident angle between the incident shock front and the reflecting surface (Peng, 2009). The oblique reflection and Mach stem reflection occur when the incident angles are less than 40° and greater than 40° respectively.

Thus, for this study case the reflection of blast wave is when the incident blast wave strikes a stiff surface such as open surface with no barrier of wall at all or a front of the barrier of wall, it is reflected. Figure 2.3 below shows the pattern of the reflected wave in the outward movement of the spherical blast wave originating from an air burst. Remennikov (2007) stated that in the first stage, the wave front has not reached the ground; the second stage is somewhat later in time, and in the third stage a reflected wave, indicated by the dashed line, has been produced.
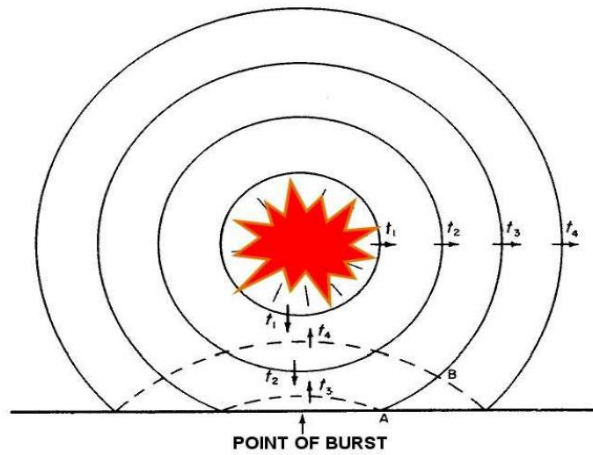
Figure 2.3 The pattern of the reflected wave in the outward movement of the spherical blast wave

2.1.1.1 *Without an Obstruction of Wall*

In the free-field blast pressure wave, within a high explosive the supersonic detonation forms gases that experience intense expansion which cause the surrounding layer of air compressed and form a blast wave. Therefore, the blast wave will expand out from the explosive charge in a high-pressure wave front. In a free-field application, this blast wave propagates along the surface until it is no longer supersonic (Rouse and Consultants, 2012). Otherwise, when the vehicles respond directly to the blast, it will result in vehicle movement, occupant injuries and fatality.

Besides that, the detonation wave was created when the blast occurs nearly to vehicles such as car by its detonating explosive and it will give the bad impact to the vehicles and its occupants. The minimum safe distance, which is the distance at which the probability of failure approaches zero, ranges from about 7m for a car to about 20m for a semi-trailer (Thomas et al., 2018). So, the standoff distance has a significant effect on structural reliability for all vehicles classes and may one of the greatest importance for the blast events worst occur.

However, Yang et al. (2013) shows that as the detonation wave comes in contact with, for example, the metal vehicle body, it transfers a pressure pulse, or shock wave, to the metal body. Besides that, the impedance matching can determine the pressure level of the shock wave in the metal material. The interaction between the shock wave and the surface side of the vehicle body will cause the acceleration of the shock front

11

and a reflected shock. This process continues until the shock wave and its reflected waves interact with the occupants in the vehicles as the human body experiences rapidly changing loads, causing injuries or fatality (Yang et al., 2013).
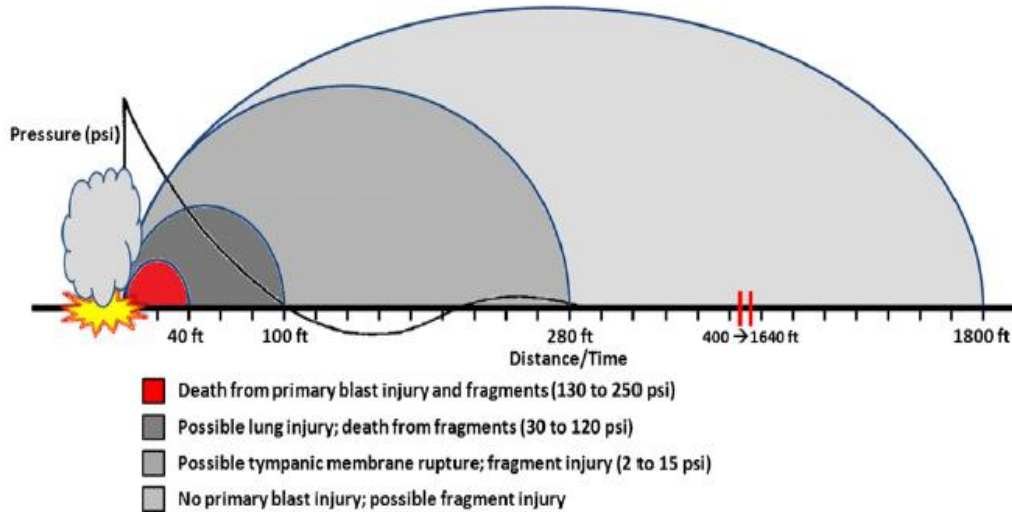
Figure 2.4 Illustration of Friedlander curve with maximum effective radius of primary and secondary blast injuries of an open spaced without any barrier wall, 155-mm mortar shell explosion with 200 lbs. (100 kg) of TNT equivalent

Source: Kang, Lehman and Carragee (2012).

Kang, Lehman and Carragee (2012) reported that in an open space environment, the nearly instantaneous peak in ambient air pressure quickly decays as it travels away from the explosion epicentre through a well-defined pressure or time curve called a ''Friedlander wave'' whereas when in an enclosed space, this typical relationship does not occur, as blast waves deflect, reflect, and coalesce, which can magnify the destructive power eight to nine times and cause significantly greater injury.

In addition, one of the important factors that effect to the magnitude of the blast overpressure is the distance from the blast event. The greater the blast overpressure as the closer the object to an explosion. Wolf et al. (2009) states that if the distance from an explosion is doubled, the peak overpressure will decrease to one-eighth of the original value. He also showed that one kilogram explosive might cause the blast overpressure more than 500 kPa at the centre of the detonation. So, possibly no worst injury can occur if the object located 3m from the detonation point because the blast overpressure could be as little as 20 kPa.

2.1.1.2   *With an Obstruction of Wall*

In the previous sub-topic was discussed about the interaction of the blast wave in open space which there is no obstruction at all but when the structure is introduced such as the barrier wall, the blast wave will change it way. Peng (2009) discussed that the way to enhance the survivability of structures to blast loads is to provide a blast barrier at the blast parameter event. This is because when a charge from the blast wave impacted the barrier wall, the blast wave will diffract and reflect around or over the barrier wall as shown in figure 2.5. This is because in most cases, majority of the blast wave not being absorbed or transmitted over the barrier but it being reflected around it. Thus, the existing of this barrier, some part of the blast wave is reflected back from the way it came as well as wrapping around the top of the barrier (Theses and Baumgart, 2014). Therefore, the blast barrier can effectively protect buildings against air blast wave from high explosives (Peng, 2009).

For example, the attack on the U.S. Embassy Annex in 1984, in Antilias, East Beirut has used 2.8 tons of explosives with only 11 deaths were recorded and the injured rate were relatively low. According to this case, the car bomb was detonated on a sunken road approaching the Annex car park, and a small retaining wall provided some shielding to the blast at a standoff distance from the embassy (Rouse and Consultants, 2012). Contrarily with the case in 1983 at the U.S Marine Corps Battalion Headquarters in Beirut, 5.5 tons of explosives were denoted. The explosion has been demolished the concrete building and over 300 people were killed and injury in that attack. From this two different scenarios, it can be concluded that with the present of the barrier wall, it can reduce the fatality effect to the civilian nearby. Zhou and Hao, (2009) also stated that that the simplest way to enhance the survivability of these structure and the vehicle nearby such as car to blast loads is by providing a blast barrier at that perimeter. This is because it can acts as an obstacle in the direction of the blast wave propagation (Zhou and Hao, 2009).

In addition, the wave is lessened for some distance behind the wall. According to Rouse and Consultants (2012), the area where the wall affects the blast pressures and causes a pressure reduction is defined as the shadow area on the backside of the wall. It is better to have higher wall height than increasing the standoff distance which it will

affect the shadow region. This is because of the laws of sound propagation, which state, the pressure drops by a factor of ten when the distance from the source doubles (Theses and Baumgart, 2014).
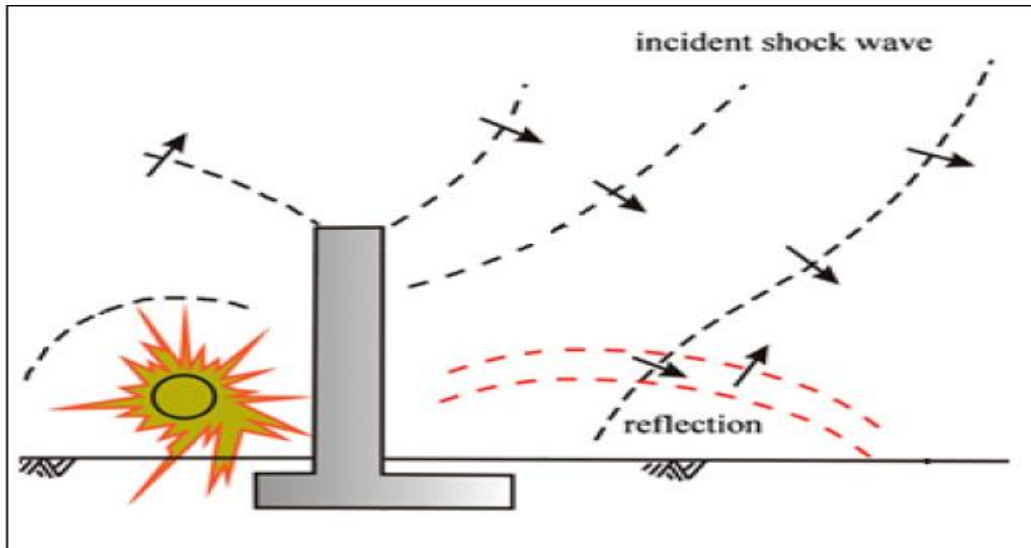
Figure 2.5 The diffraction of the blast wave over the barrier.

According to the Rouse and Consultants (2012), the barrier walls serve two purposes which are they ensure that an explosive charge is set at a standoff distance away from the vehicles and the surrounding and up to a point, they diffract blast waves to mitigate the full force of the blast pressures on the protected object. So, it means that to mitigate the explosive damage form the detonation of an explosive charge to target structures which are the vehicles nearby, the barrier walls can be constructed to ensure the safety of civilians. On the other hand, it was found that a barrier between an explosion and a building can not only reduce the peak reflected pressure and impulse on the surface of the building, but also delay the arrival time of the blast wave (Zhou and Hao, 2009).

Besides that, it has been demonstrated in experimental results and numerical simulations as the barrier is the one of the effective ways to reduce blast load. So, it acts as an obstacle in the propagation of the blast wave towards the object. Therefore, some portion of the explosive energy is reflected back, and then the distribution of the blast pressure on the structure behind the barrier is changed and the peak pressure is reduced (Zhou and Hao, 2009). When the pressure is reduced, it will provide standoff distance that can protect the vehicles from extremely external explosion and can decrease the

14

rate of fatality. One of the suggestion or the best way to protect any object nearby the blast event which is the vehicles is by increase the standoff distance. However, this can be achieved through the installation of barrier structures (Thomas et al., 2018).

2.2.3 Blast Impact on Human

The blast injuries are a wide range of explosion related to the explosive devices. These injuries are one of the most debilitating and lethal wounds from the blast event caused by penetrating fragments from the vehicle material, projectile glass from broken window or complete destruction of the vehicle. However, the characteristics of the injuries have been difficult to predict and generalize because the variable severity and spectrum of injury with each attack is largely related to the explosive weight and material, as well as the preparation and detonation technique of the blast (Kang et al., 2012). Therefore, there are four types of blast injuries that are related to this blast event which are primary, secondary, tertiary and quaternary injuries.

Besides, when explosive device exploded, the explosive material will undergo a rapid exothermic chemical reaction by transforming the explosive material from liquid or solid to a gas, it releases a significant amount of stored potential energy. This detonation product will compress it superheated gas then it rapidly expands with the pressure from 1.4 to 3 million psi and the temperature from 2,000˚C to 6,000˚C. According to the Kang, Lehman and Carragee (2012), this gas expansion then instantaneously compresses the surrounding ambient air, forming a blast wave that propagates supersonically and radially from the detonation site. Thus, when the high compressed air interacts with the human body this will cause primary blast injury and it usually referred as overpressure injuries.

The injury pattern in this primary blast occur are varies according to the different impact of pressure:

Table 2.2 Injury pattern with different pressure.

Injury Pattern	Effective Overpressure (kPa)
Auditory shift[1]	14
Rupture eardrum in about 1 percent of subjects[2]	34
Tympanic membrane rupture[1]	34 to 103
Threshold of lung damages[2]	103
Lung injury, pneumothorax, air embolism, intestinal emphysema[1]	206 to 552
Eardrum rupture in about 99 percent of all subjects[2]	310
Threshold of fatalities[2]	234 to 310
99 percent of fatalities[2]	379 to 448
100 percent of fatalities[2]	450 and above

Source: Kang, Lehman and Carragee[1] (2012) and Zipf, Kenneth and Cashdollar[2] (2010).

Kang, Lehman and Carragee, (2012) compared the effects of explosions occurring in a vehicle with those outside a vehicle. He found that the risk of overpressure injuries is reduced when inside a vehicle as a 17 kg explosive is detonated 3m away. The result is the peak overpressure outside a vehicle is approximately 28 times than inside the vehicle a 50% chance of death. Thus, from primary blast injury (Table 2.2), if the person inside the vehicle are exposed to an overpressure of 34 kPa, he may result in tympanic membrane rupture whereas outside the vehicle and protected from fragment injury would likely experience an overpressure of 432 kPa, which can result in lung injury, pneumothorax, air embolism and intestinal emphysema (Kang, Lehman and Carragee, 2012).

Besides that, Zipf, Kenneth and Cashdollar, (2010) stated that the rupture of eardrum in about 1% of subjects occurs at about 34 kPa blast overpressure while for 310 kPa of blast overpressure will cause eardrum rupture eardrums in about 99% of all subjects. A 103 kPa blast overpressure will cause the threshold for lung damages. In addition, 234 kPa to 310 kPa overpressure may cause 1% fatalities, and 379 kPa to 448 kPa overpressure may cause 99% of fatalities. Table 2.2 shows the effect on the human body with the different blast overpressure.

Moreover, according to the Malhotra, Carson and McFadden, (2017), the direct effect on humans due to an explosion is the sudden increase in pressure caused by the blast wave which can cause severity injury to human organs such as ears and lungs. The first injury is the ear damage. All know that the ear is very sensitive to air pressure and it responds to even very small variation in air pressure. Thus, the minimum ear drum rupture is about 34 kPa of blast overpressure, but at lower level of overpressure than 34 kPa, the temporary hearing loss can occur. Next is about lung damage. It can happen when the external blast pressure on the chest wall becomes larger than the internal pressure, that will cause the chest wall moves inwards. However, when the duration of the blast is very long, the lung damage can cause at pressures much lower than stated in table 2.3 below. Table 2.3 shows the details of injury of the ear and lung damage.

Table 2.3 Human ear and lung damage due to blast overpressure.

Type of Damage	Effective Overpressure(kPa)
Threshold of eardrum rupture	34
50 percent ruptured eardrums	325 and above
Threshold of lung injury	210 to 280
50 percent damaged lungs	510 and above
Threshold of lethality	700 to 850
50 percent lethality	900 to 1300
Near 100 percent lethality	1400 and above

Source: Malhotra, Carson and McFadden (2010).

2.3   AUTODYN

Currently, an expensive actual blast test has been replaced with an alternative method which is the numerical simulation of ANSYS AUTODYN. The AUTODYN is an integrated explicit analysis tool program specially designed for modelling non-linear dynamic problems that uses finite elements (FE), finite volume (CFD) and mesh-free particle (SPH) to solve nonlinear dynamic problems of solid, fluids, gas and the interaction between them (Ali et al., 2015). The Arbitrary Lagrange Euler (ALE) method is used as a numerical approach for the interface analysis between the air and structure that allows different part of the solvers such as structure, fluids and gases. Therefore, this method can be modelled simultaneously using Lagrange and

Euler method. Besides, for solving the blasting interaction problem, the Eulerian method is used. This method is used in modelling large deformation zone with simple geometry whereas for modelling the complex structure, the Lagrangian method is used. Thus, these different solvers are coupled together in space and time.

Besides that, AUTODYN also offers multi-solver coupling for multi-physic including coupling between FE, CFD and SPH. The material model used in AUTODYN are subjected to the RC wall, blast load, air domain and simplified vehicle. The used of that materials are to consider the strain rate effects and the appropriate coupling between air-solid interface. The default material in AUTODYN such as CONC-35MPA and STEEL 4340 is assigned for concrete and steel. The material for concrete and steel is based respectively on the material model of Riedel, Hiermayer and Thoma (RHT) and the material model of Johnson-Cook (JC). Moreover, the ideal gas expression of state (EOS) is used for the air domain while the standard model of TNT modelled by Jones-Wilkins-Lee (JWL) EOS is used. Lastly, the entire body of the vehicle material and the window are used with aluminium alloy and glass respectively for the simplified vehicle.

2.3.1   Material Model for Concrete

In this study, the material model developed by Riedel, Hiermayer and Thoma (RHT) is adopted in this study. The RHT concrete model for brittle materials is an advanced plasticity model. The model includes pressure hardening, strain hardening, strain rate hardening, compressive and tensile meridian third invariant dependence as well as strain softening damage model. This model also uses the ρ-α state equation (Herrman, 1969) to represent the thermodynamic behaviour of concrete at high stress, providing a reasonably detailed description of compaction behaviour at low stress ranges. It is established that at the same pressure and temperature the specific internal energy for the porous material is the same as the solid material. The model consists of three pressurized surfaces, a fracture surface, an elastic limit surface and a residual strength surface for the crushed material. Figure 2.6 shows these strength surfaces.
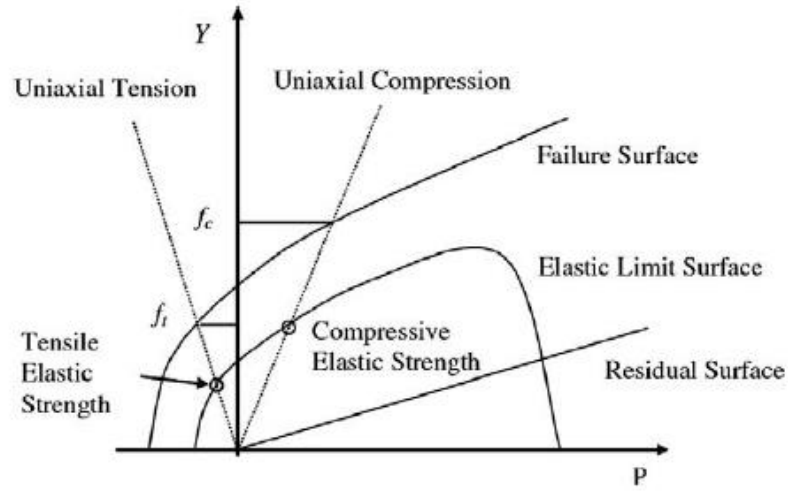
Figure 2.6 Maximum strength, yield strength and residual strength surfaces.

Source: ANSYS (2011)

The failure surface, Y_{fail} is defined as a function of the normalised pressure p*, load angle θ and strain $\acute{\epsilon}$;

$$Y_{fail} (p^*, \theta, \acute{\epsilon}) = Y_c(p^*) \cdot r_3 (\theta) \cdot F_{rate}(\acute{\epsilon}) \qquad 2.1$$

where $Y_c(p^*)$ is the comprehensive meridian and it is representing by

$$Y_c(p^*) = f_c [A \cdot (p^* - p^*_{spall} F_{rate} (\acute{\epsilon}))^N] \qquad 2.2$$

where, f_c denotes the material uniaxial compressive strength; A is failure surface; N is failure surface exponent; $p^* = p/ f_c$ is normalised pressure and $p^*_{spall} = f_t/f_c$, where f_t is the material uniaxial tensile strength; $F_{rate} (\acute{\epsilon})$ represents the dynamic increase factor (DIF) as a function of strain rate $\acute{\epsilon}$. $r_3 (\theta)$ defines the third invariant model dependence as a function of the second and third stress invariant and a force ratio at zero Q_2. Figure 2.7 shows the tensile and comprehensive meridian on the π plane of stress.
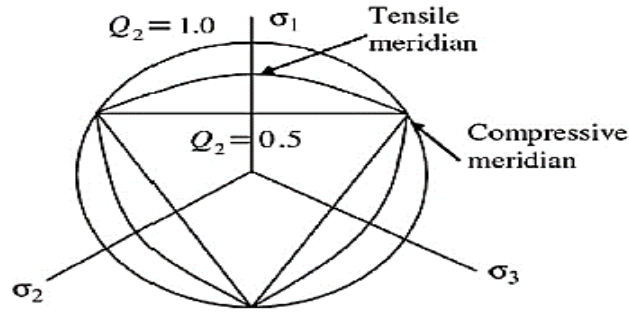
Figure 2.7 Third invariant depend on stress plane.

Source: ANSYS (2011)

The elastic limit surface is scaled from the failure surface,

$$Y_{elastic} = Y_{fail} \cdot F_{elastic} \cdot F_{cap} (p) \qquad 2.3$$

where $F_{elastic}$ is the ratio of the elastic strength to failure surface strength. $F_{cap}(p)$ is a function that limits the elastic deviatoric stresses under hydrostatic compression, varying within the range of (0,1) for pressure between initial compaction and solid compaction pressure.

The residual failure surface is defined as

$$Y^*_{residual} = B \cdot (p^*)^M \qquad 2.5$$

where B is the residual failure surface constant, and M is residual failure surface exponent.

Following the hardening phase, additional plastic straining of the material results in damage and strength reduction. Damage is assumed to accumulate using the relationship

$$D = \sum \frac{\Delta \varepsilon_\rho}{\varepsilon_\rho failure} = \sum \frac{\Delta \varepsilon_\rho}{D_1 (\rho^* spall) d2} \qquad 2.1$$

where D_1 and D_2 are material constants for effective strain to fracture.

The damage accumulation can have two effects in the model, reduction in strength and reduction in shear stiffness as below

$$Y^*_{fracture} = (1 - D)Y^*_{failure} + DY^*_{residual} \qquad 2.6$$

$$G_{fracture} = (1 - D)G_{elastic} + DG_{residual} \qquad 2.7$$

where $G_{elastic}$, $G_{residual}$ and $G_{fracture}$ are the shear modulus.

2.3.2 Material Model for Steel Reinforcement

A Johnson-Cook (JC) material model (Johnson and Cook, 1983) was used to describe the steel reinforcement behaviour. This model represents the strength behaviour of material subject to high strain, high strain rates, and typically metal high temperature. The model defines the yield stress Y as

$$Y = \lfloor A + B\varepsilon_p^n \rfloor \left\lfloor 1 + CIn\frac{\varepsilon_\rho}{\varepsilon_0} \right\rfloor \lfloor 1 - T_H^m \rfloor \qquad 2.8$$

where

ε_p is effective plastic strain, $\varepsilon_{p=} \varepsilon / \varepsilon_0$ is normalised effective plastic strain rate for $\varepsilon_0 = 1s^{-1}$

homologous temperature which is $T_H = (T - T_{room}) / (T_{melt} - T_{room})$ where T_{room} is room temperature and T_{melt} is melting temperature

A, B, C, m, n are materials constant. The first, second and third brackets in the above equation, respectively, represent stress as a function of strain, strain rate effect on yield strength and thermal softening. The constant is the basic yield stress at low stress, while the effect of strain hardening is represented by B and n.

2.3.3 Material Model for Air and High Explosive

The Arbitrary Lagrange Euler (ALE) is the numerical approach to the air-structure interface analysis. By using this approach, Lagrange and Euler approaches can simultaneously model different parts of the solvers such as structure, fluids and gases. Then in space and time, these different solvers are coupled. An ideal gas EOS, which is one of the simplest forms of EOS, models air in the numerical model. The energy-related pressure is given by

$$p = (\lambda - 1) \rho e \qquad\qquad 2.9$$

where

λ = ratio of specific heat (λ = 1.4)

ρ = air density

e = specific internal energy (2.068×10^5 kJ/kg)

The AUTODYN material library's standard air constants (ANSYS, n.d.) are used in the simulation. TNT high explosives are typically modelled by the Jones-Wilkins-Lee (JWL) EOS, which models the pressure generated by chemical energy and can be shown as follows

$$P = A\left(1 - \frac{\omega}{R_1 V}\right)e^{-R_1 V} + B\left(1 - \frac{\omega}{R_2 V}\right)e^{-R_2 V} + \frac{\omega E}{V} \qquad\qquad 2.10$$

where

P = detonation pressure of high explosive

V = specific volume

E = specific internal energy

(A, B, R1, R2 and ω are material constant)

2.3.4 Material Model for Glass and Aluminium Alloy

The glass model was modelled with the Johnson Holmquist Strength Continuous model (Yusof et al., 2014). Holmquist developed this material model in 1995 and hence namely JHS model. This is the standard float glass material model in AUTODYN's material library that describes float glass behaviour. Both the strain rate effect and the

material damage are considered by the JHS model. The equation of float glass strength was displayed in equation below.

$$\sigma^* = \sigma_i^* - D(\sigma_i^* - \sigma_f^*)$$ 2.11

where

σ^* = the strength of glass
σ_i^* = normalized intact strength
σ_f^* = normalized fracture strength
D = damaged scalar

Besides that, the material model for the simplified vehicle also used the JC strength model (Marx et al., 2019), which was well explained in equation 2.8.

2.4   Summary

Several studies about numerical analysis of the blast pressure on the vehicle with and without the wall as a barrier through journals, books, internet and articles are discussed in this chapter. As all know, when the explosion occurs, it emits the blast wave in high pressure which can destroy the vehicles nearby and people surrounding. If the vehicles respond directly to the blast, occupant injury and fatality will result. Peng (2009) discussed that, by providing a blast barrier at the blast parameter event is the way to enhance the survival of the civilian nearby and the structure of the vehicle to blast loads. In addition, according to the Thomas et al., (2018) one of the suggestion or the best way to protect any object such as vehicles nearby the blast event is by increase the standoff distance through the installation of barrier structures. Hence, ANSYS AUTODYN numerical simulation is used to achieve the objectives of this study, which is replaced the costly actual blast test.

CHAPTER 3

METHODOLOGY

3.1   Introduction

This chapter describes the current sequence of research methodology as shown in figure 3.1. The main objective of this research is to determine the blast overpressure on the vehicle with and without wall as a barrier. The first part presents the analysis of blast overpressure parameters in the AUTODYN 3D non-linear FE software package using the Friedlander equation and Arbitrary Lagrange Euler (ALE). It is used due to its ability to integrate Lagrangian and Eulerian techniques, allows for the possible assessment of blast overpressure and its impact on the simplified vehicle structure. The numerical simulation initially conducted in 3D free air explosion in 1000 mm x 1000 mm x 5500 mm volume of air for case 1. Besides that, the validation numerical modelling of 13.61 kg (30 lbs.) TNT of the gauge located at 18 ft. from the charge weight will be verified by the blast test on the RC wall available in previous literature by Yan et. al, (2011). If the result is verified, the remapped of the same blast wedge into the air volume at different condition according to the cases involved in this study which is in the free field, with and without wall as a barrier. This chapter also discusses the details of the model used for the reinforced concrete wall (RC wall), steel reinforcement, air domain, TNT and the simplified vehicle.
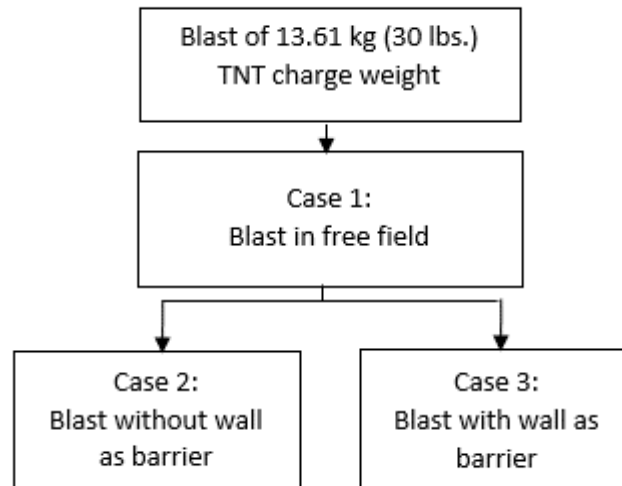
Figure 3.1 Flowchart for methodology

3.2 Numerical Modelling RC Wall and Simplified Vehicle Subjected to Blast Load in AUTODYN

AUTODYN is an integrating amongst Lagrangian and Eulerian technique that allows the possible valuation of the blast pressure and its impact on the structures such as vehicle and wall in the current study. Figure 3.2 shows the ALE (Arbitrary Lagrange Euler) solver is used as for the mesh hybrid between Lagrangian and Eulerian method.
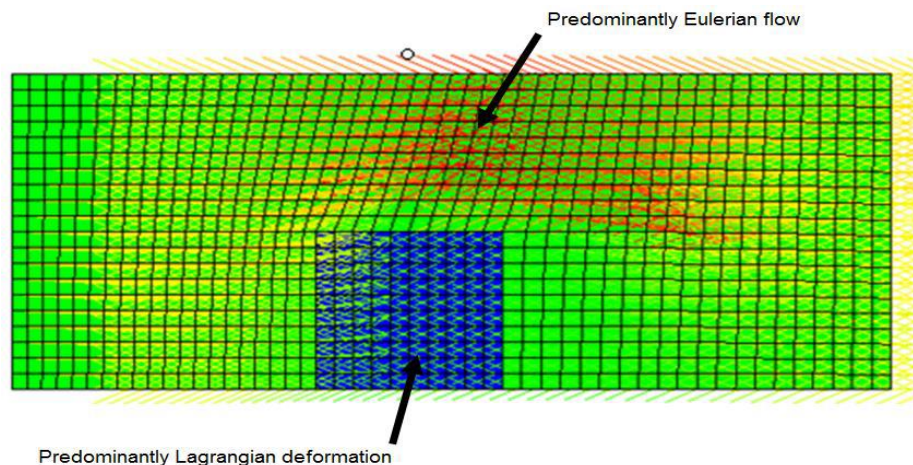

Figure 3.2 ALE solver technique in AUTODYN

Source: ANSYS (2011)

Besides, the identification of solid elements used is performed in ANSYS-Workbench before the RC wall is exported into AUTODYN solver for blast and analysis impact. The reinforced concrete wall was reinforced with 16 mm diameter on vertical reinforcement and 10 mm diameter on transverse stirrups, both at 150 mm spacing. The concrete cover on all sides of the walls is 25 mm thick. The cylinder compressive strength of the concrete is 44 MPa with standard deviation of 1.38 MPa; the Modulus of Elasticity is 31.5 GPa with a standard deviation of 827 MPa. The reinforcement had yield strength of 619 MPa and Young's modulus of 200 GPa. Figure 3.3 shows the geometry and section detail of the wall. The walls have a cross-sectional dimension of 1219 mm × 1219 mm with wall thickness of 150 mm and 305 mm thickness of footing.
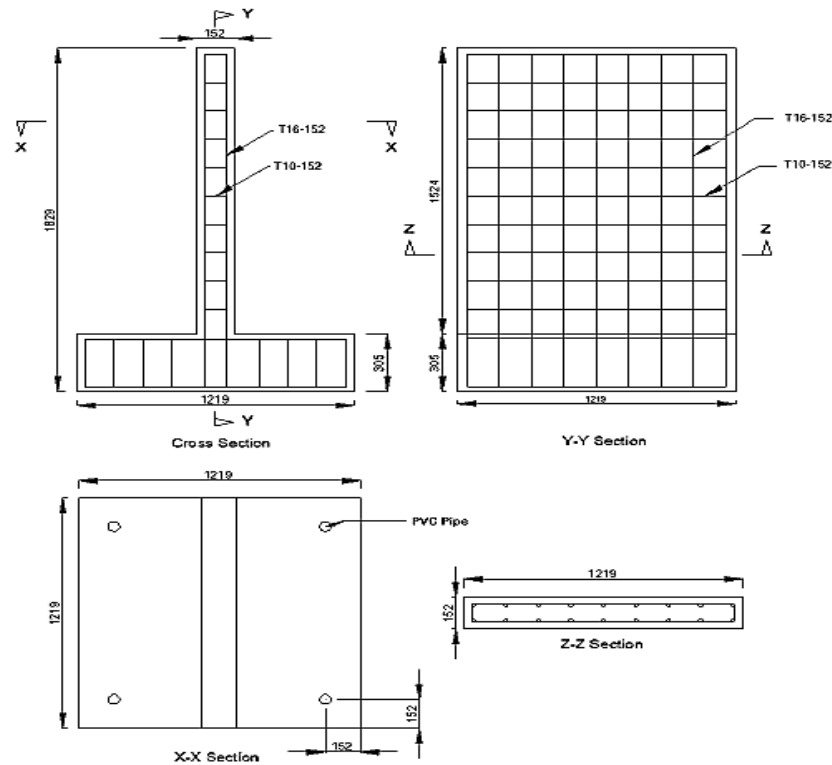

Figure 3.3 Details of the RC wall (Unit: mm)

Source: Chen et al., (2008) and Yan et al., (2011)

Furthermore, to simulate those 2 cases, the simplified type of vehicle model used in AUTODYN simulation is the typical car size with the length of 4160 mm, the width of 1690 mm and the height of 2530 mm as shown in figure 3.4.
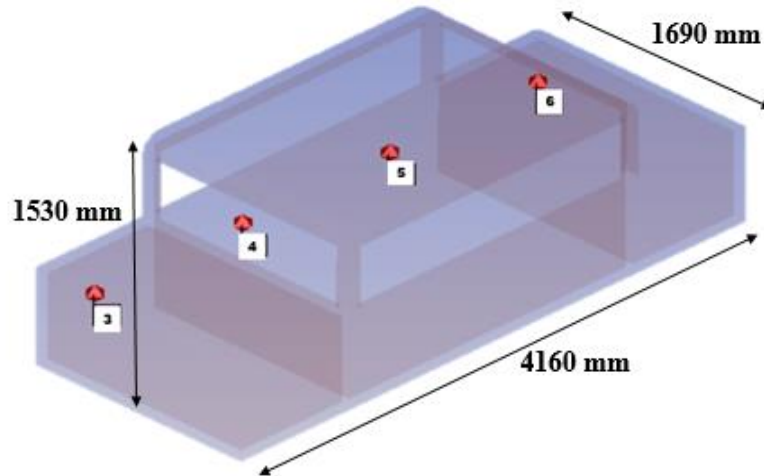
26

Figure 3.4 Details of the simplified vehicle

The initial detonation of the explosive and blast wave propagation is modelled with an axial symmetric in wedge shape. The used of this wedge is to apply the effect of explosion in 3D model. This wedge is filled with 150 mm radius of 13.61 kg (30 lbs.) of TNT material model and the remaining area outside the circle is filled with air material model as shown in figure 3.5. After that, the detonation is run until the blast wave reached at 1000 mm from the centre of detonation as shown on figure 3.6. The ' fill ' file consists of the blast overpressure history being created and the same blast wedge was remapped and used into the air volume at different cases which are for case 1; blast in open space, case 2; without wall as barrier and for case 3 with wall as barrier.
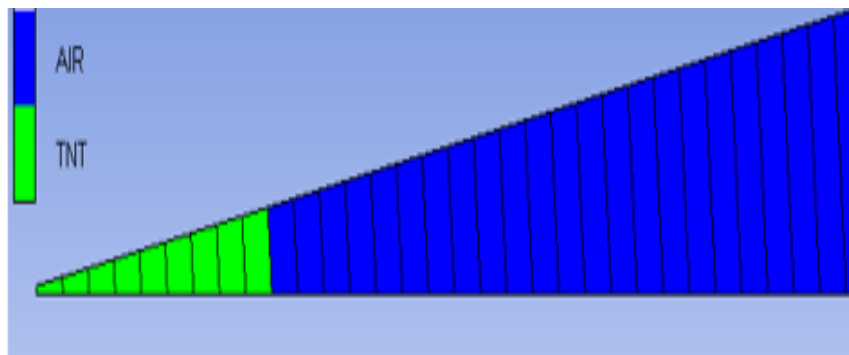

Figure 3.5 1000 mm of wedge in 2D filled with air and TNT
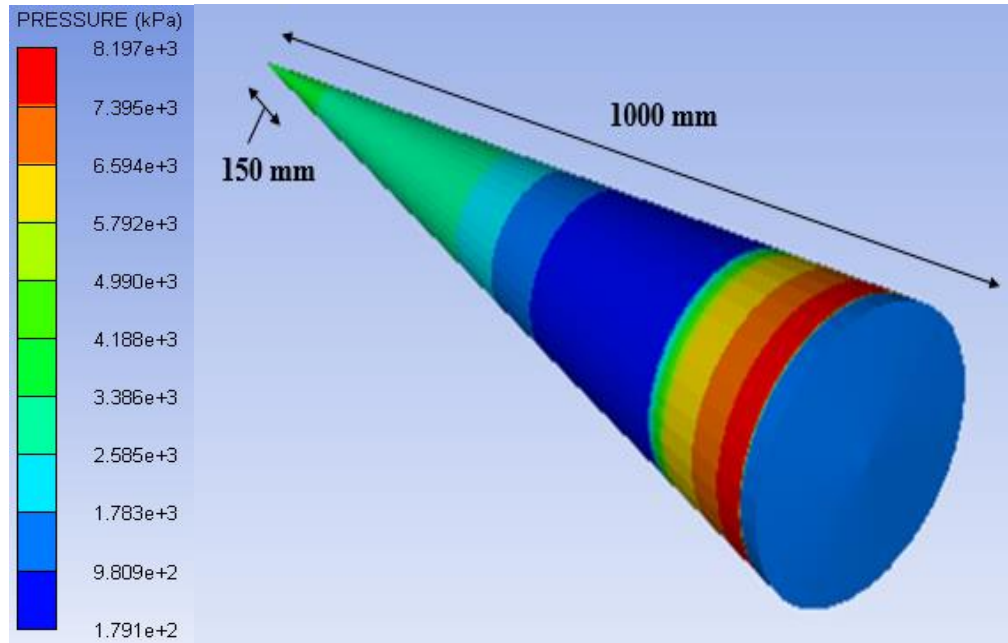
Figure 3.6 Blast wedge in 3D during solving progress with pressure contour for 30 lbs. TNT

Table 3.1 show the example of material model for all the materials used in AUTODYN. The standard material used for concrete of RC wall is concrete-35 MPa. The material model was developed by Reidel, Hiermayer and Thoma (RHT). However, the standard material model for steel used in RC wall is steel 4340. This material model was developed by Johnson and Cook (JC). In addition, the ideal gas expression of state (EOS) is used to describe the air behaviour modelled for the air domain while the standard model of TNT modelled by Jones-Wilkins- Lee expression of state (EOS) is used to describe the behaviour for the blast load. Lastly for simplified vehicle, the whole body of the simplified car is by aluminium alloy and the window of the car is by the glass. The material properties are listed in tables subjected to all material used in numerical simulation.

Table 3.1 Material Model in AUTODYN

Material		Material Model in AUTODYN
RC Wall	Concrete	-Reidel, Hiermayer and Thoma (RHT) concrete strength (CONC-35 MPa)
	Steel	-Johnson and Cook (JC) Strength (STEEL 4340)
Blast Load	TNT	-Jones-Wilkins-Lee Expression of State (JWL EOS)
Air Domain	Air	-Ideal Gas EOS
Simplified Vehicle	Body	-Aluminium Alloy
	Window	-Glass

Table 3.2 Employed material data for concrete, input to the RHT model.

Equation of state	Ideal Gas
Reference density	2.75000E + 00 (g/cm3)
Porous density	2.31400E + 00 (g/cm3)
Porous soundspeed	2.92000E + 03 (m/s)
Initial compaction pressure	2.33000E + 04 (kPa)
Solid compaction pressure	6.00000E + 06 (kPa)
Compaction exponent	3.00000E + 00 (-)
Solid EOS	Polynomial
Bulk modulus A1	3.57200E + 07 (kPa)
Parameter A2	3.95800E + 07 (kPa)
Parameter A3	9.04000E + 06 (kPa)
Parameter B0	1.22000E + 00 (-)
Parameter B1	1.22000E + 00 (-)
Parameter T1	3.52700E + 07 (kPa)
Parameter T2	0.00000E + 00 (-)
Reference temperature	3.00000E + 02 (K)
Specific heat	6.54000E + 02 (J/kgK)
Compaction curve	Standard
Strength	RHT concrete
Shear modulus	1.67000E + 07 (kPa)
Compressive strength (f_c)	3.50000E + 04 (kPa)
Tensile strength (f_t/f_c)	1.00000E - 01 (-)
Shear strength (f_t/f_c)	1.80000E - 01 (-)
Intact failure surface constant A	1.60000E + 00 (-)
Intact failure surface exponent N	6.10000E - 01 (-)
Tens./Comp. meridian ratio (Q)	6.80500E - 01 (-)
Brittle to ductile transition	1.05000E - 02 (-)
G (elastic)/(elastic-plastic)	2.00000E + 00 (-)
Elastic strength/f_t	7.00000E - 01 (-)

Table 3.2 Continued

Elastic strength/f_c	5.30000E - 01 (-)
Fractured strength constant B	1.60000E + 00 (-)
Fractured strength exponent M	6.10000E - 01 (-)
Compressive strain-rate exponent a	3.20000E – 02 (-)
Tensile strain-rate exponent	3.60000E – 02 (-)
Max. fracture strength ratio	1.0000E + 20 (-)
Use CAP on elastic surface?	Yes
Failure	**RHT concrete**
Damage constant D1	4.00000E - 20 (-)
Damage constant D2	1.00000E + 00 (-)
Minimum strain to failure	1.00000E - 02 (-)
Tensile failure	1.30000E – 01 (-)
Principal tensile failure stress	Principal stress
Max. principal stress difference/2	3.50000E + 03 (kPa)
Crack softening	1.01000E + 20 (kPa)
Fracture energy, Gf	Yes
Flow rule	Bulking (Associative)
Stochastic failure	No
Erosion	**Geometric strain**
Erosion strain	2.00000E + 00 (-)
Type of geometric strain	Instantaneous

Table 3.3 Employed material data for reinforcement steel

Equation of state	**Ideal Gas**
Reference density	7.83000E + 00 (g/cm3)
Bulk modulus	1.59000E + 08 (g/cm3)
Reference temperature	3.00000E + 02 (K)
Specific heat	4.77000E + 00 (J/kgK)
Thermal conductivity	0.00000E + 00 (J/mKs)
Strength	Piecewise JC
Shear modulus	8.18000E + 07 (kPa)
Yield stress (zero plastic strain)	5.49330E + 05 (kPa)
Eff Plastic strain #1	6.70000E - 03 (-)
Eff Plastic strain #2	1.62000E - 02 (-)
Eff Plastic strain #3	2.86000E - 02 (-)
Eff Plastic strain #4	4.57000E - 02 (-)
Eff Plastic strain #5	6.45000E - 02 (-)
Eff Plastic strain #6	9.21000E - 02 (-)
Eff Plastic strain #7	1.27800E - 01 (-)
Eff Plastic strain #8	1.79200E - 01 (-)
Eff Plastic strain #9	1.79201E - 01 (-)
Eff Plastic strain #10	1.00000E + 01 (-)
Yield stress #1	5.62000E + 05 (kPa)
Yield stress #2	5.68000E + 05 (kPa)

Table 3.3 Continued

Yield stress #3	6.27000E + 05 (kPa)
Yield stress #4	6.78000E + 05 (kPa)
Yield stress #5	7.15000E + 05 (kPa)
Yield stress #6	7.46000E + 05 (kPa)
Yield stress #7	7.76000E + 05 (kPa)
Yield stress #8	7.95000E + 05 (kPa)
Yield stress #9	7.95000E + 05 (kPa)
Yield stress #10	7.95000E + 05 (kPa)
Strain-rate constant C	0.00000E + 00 (-)
Thermal softening exponent m	0.00000E + 00 (-)
Melting temperature	0.00000E + 00 (K)
Ref. strain-rate (1/s)	1.00000E + 00 (-)
Failure	None
Erosion	None

Table 3.4 Employed material data for air, input to the ideal gas EOS

Equation of state	**Ideal Gas**
Reference density	1.22500E+00 (kg/m3)
Specific heat	7.17600E+02 (J/kgC)
Adiabatic exponent γ	1.40000E+00 (none)
Reference temperature	1.50500E+01 (c)
Specific internal energy	2.00000E+05 (J/kg)

Table 3.5 Employed material data for TNT, input to the JWL EOS

Equation of state	**JWL**
Reference density	1.63000E+00 (g/cm^3)
Parameter A	3.73770E+08 (kPa)
Parameter B	3.74710E+06 (kPa)
Parameter R_1	4.15000E+00 (none)
Parameter R_2	9.00000E-01 (none)
Parameter ω	3.50000E-01 (none)
C-J Detonation velocity	6.93000E+03 (m/s)
C-J Energy / unit volume	6.00000E+00 (kJ/m^3)
C-J Pressure	2.10000E+00 (kPa)
Strength	None
Failure	None
Erosion	None

Table 3.6 Employed material data for Aluminium alloy

Material	Property	Value
Aluminium Alloy	Shear modulus	26.7 (GPa)
	Bulk modulus	69.6 (GPa)
	Young's Modulus	71 (GPa)
	Poisson's ratio	0.33
	Density	2770 (kg/m3)
	Specific heat	875 (J/kg.^{O}C)

Table 3.7 Employed material data for Glass

Glass	Value
Density	2500.00E+00 (kg m^{-3})
Isotropic Thermal Conductivity	1.40E+00 (W m^{-1}C^{-1})
Specific Heat, Cρ	750.00E+00 (J kg^{-1} C^{-1})

3.2.1 Blast Overpressure Analysis

In this study, the similar wedge of 13.61 kg (30 lbs.) TNT is used for remap function above is cogitated in the numerical simulation of different cases which are case 1 for blast in open space, for case 2 is without wall as a barrier while for case 3 is with wall as a barrier. In this simulation, the grid arrangement of I, J, K (18, 22, 72) is considered in case 2 and case 3. For the situation that has the structure of wall as barrier, TNT charge weight is located (1219 mm) 4 ft. standoff distance from the side of the wall whereas without wall TNT charge weight is located (2590 mm) 8.5 ft. standoff distance from the first pressure transducer. For case 2 and case 3, gauge 1 was located at 1219 mm away at the front of the charge weight. In addition, gauge 2, gauge 3, gauge 4, gauge 5, gauge 6 and gauge 7 is located at 1369 mm, 2588 mm, 3807 mm, 5026 mm, 6245 mm and 7464 mm away from the centre of charge weight. For gauge 3 and gauge 8 are at the height of 1219 mm and 609.5 mm respectively from the ground level.

3.2.1.1 Air Volume Type 1 (Case 1)

The air volume type 1 is used to assess the blast overpressure of the calculated explosive (TNT charge circle) in a free field explosion without taking into consideration of the RC wall and the simplified vehicle. Figure 3.7 shows the layout of the location of gauge in case 1 and the remapped blast overpressure vectors in air volume Type 1 with air volume size on I, J, K direction of 1000 mm x 1000 mm x 5500 mm respectively. Flow out of the air is allowed at all air volume borders. Pressure transducers is located at (5486 mm) 18 ft. away from the centre of charge weight.
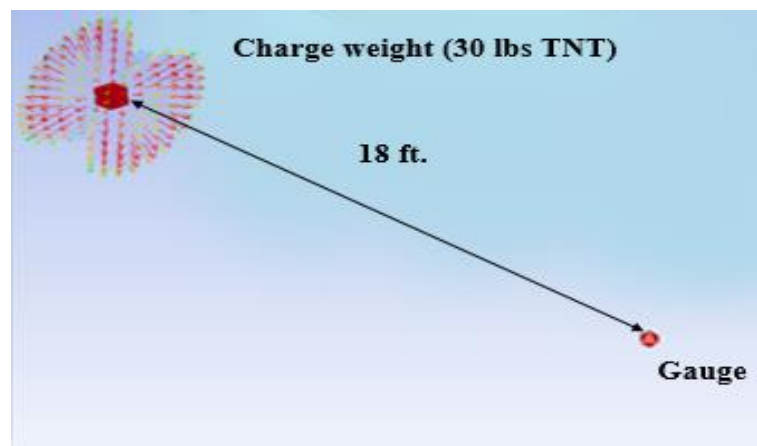

Figure 3.7 Layout of the location of gauge in case 1

3.2.1.2 Air Volume Type 2 (Case 2)

Figure 3.8 shows the 3D model and the remapped blast overpressure vectors in air volume Type 2 with air volume size on I, J, K direction of 1219 mm x 3000 mm x 1112 mm respectively with the consideration of simplified vehicle. Flow out of the air is allowed at all air volume borders. Besides that, figure 3.9 shows the location of gauges in case 2
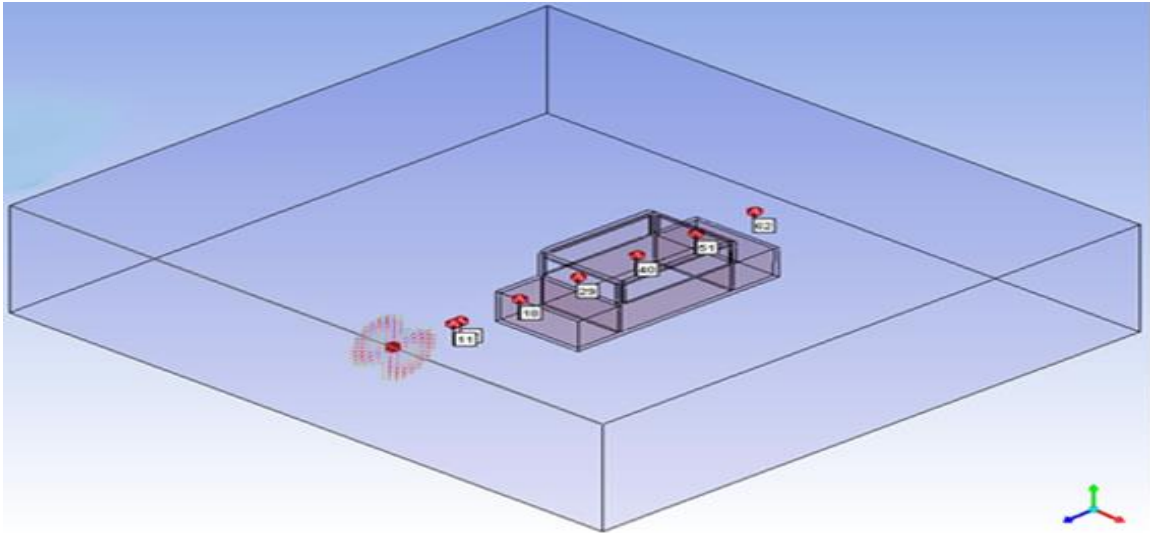
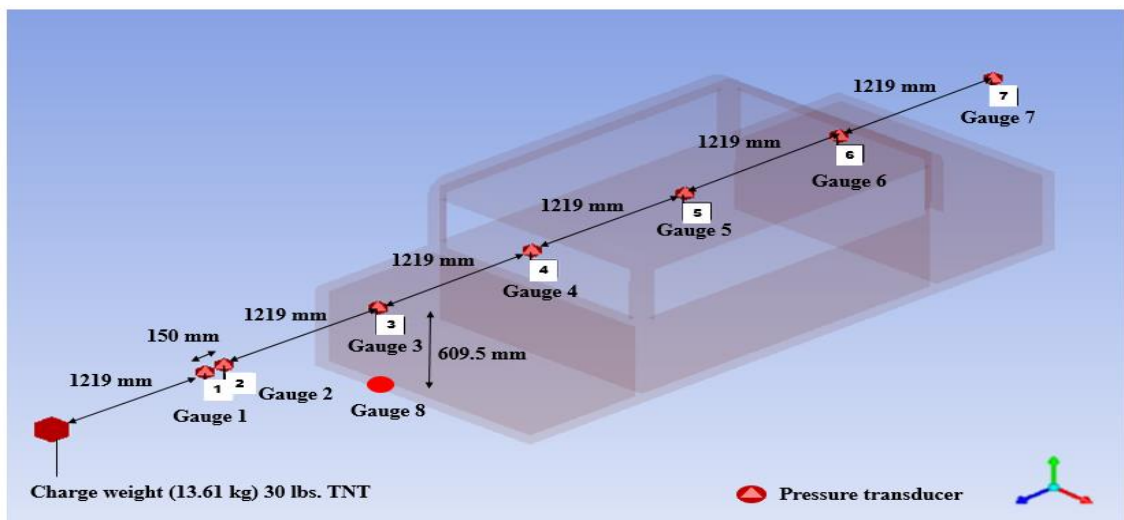Figure 3.8 Air volume type 2 for case 2

Figure 3.9 Layout of the location of gauge in case 2

3.2.1.3   Air Volume Type 3 (Case 3)

Figure 3.10 shows the 3D model and the remapped blast overpressure vectors in air volume Type 3 with air volume size on I, J, K direction of 1219 mm x 3000 mm x 1112 mm respectively with the consideration of RC wall and simplified vehicle. Flow out of the air is allowed at all air volume borders. The outflow boundaries were assigned and the flow out of air is considered on the surrounding of the structure of car and wall in symmetrical geometry which is 20 ft. on left and right side. Besides that, figure 3.11 shows the location of gauges in case 2.
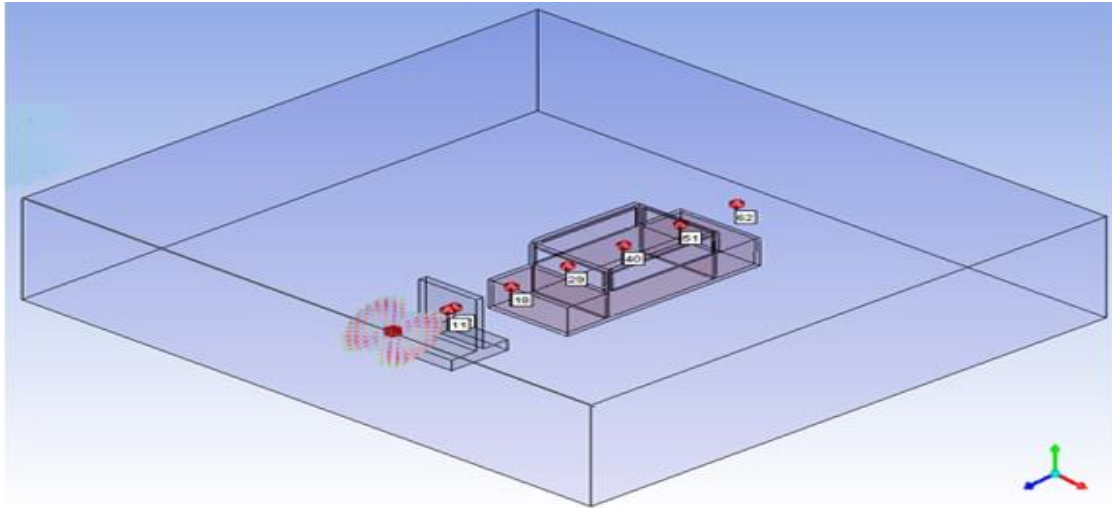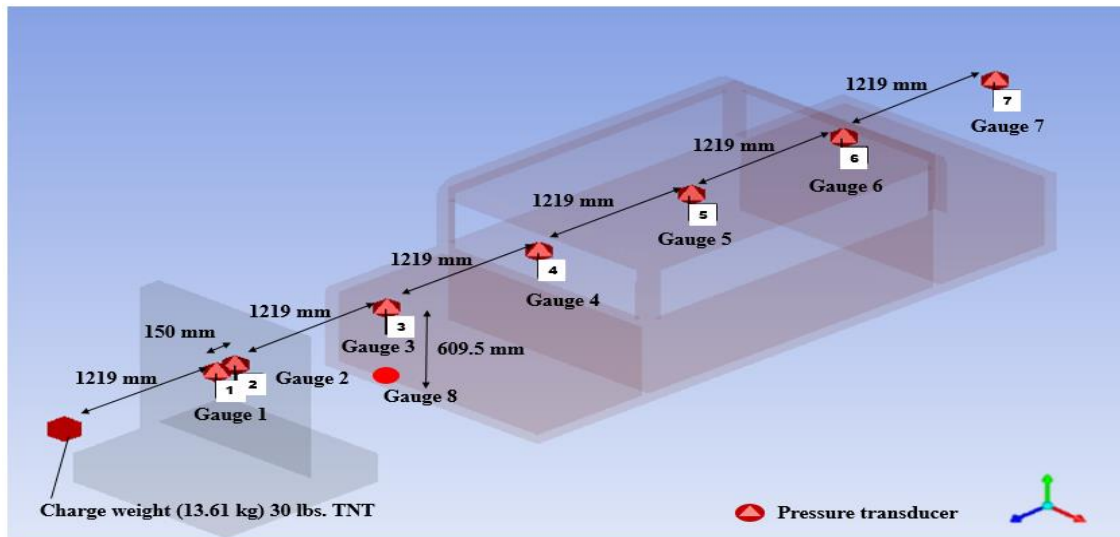
Figure 3.10 Air volume type 3 for case 3

Figure 3.11 Layout of the location of gauge in case 2

3.3　Summary

This chapter represents the flow of this current study's methodology. The numerical blast pressure 13.61 kg (30 lbs.) TNT would be assigned in three types air volume. The blast wedge will initially run in the AUTODYN and it will be documented before it can be replenished into the volume of air. Firstly, the blast pressure 13.61 kg (30 lbs.) TNT would be stimulated in the free field (Air Volume Type 1) and the reference article would validate the peak pressure (Yan et. al, 2011) before it could be

used by other parameters (Type 2 and Type 3 air volumes). The current numerical research in AUTODYN has been carried out. Besides that, Lagrangian solver was used to mesh solid for RC wall and simplified vehicle. While Eulerian solver would be used for the air. In ALE, both solvers were combined to solve the AUTODYN blast pressure.

CHAPTER 4

RESULTS AND DISCUSSION

4.1   Introduction

The principal objective of this research is to determine the blast overpressure for two different cases; with wall and without wall as a barrier. ANSYS AUTODYN is used to model and analyse the result in simulation, as well as to identify the blast pressure in the different location of the gauges. Furthermore, the peak overpressures of the gauges are also identified. This numerical simulation was conducted according to the methods discussed in methodology and the results and details analysis of data for both cases in ANSYS AUTODYN are presented in this chapter.

4.2   Blast Overpressure Analysis in AUTODYN

The following sub-chapter explain the numerically simulated blast overpressure of 13.61 kg (30 lbs.) TNT charge weight in different air volume type. From the results with the caped nodes up to 32, 000 nodes, the grid size and the proper grid arrangement on I, J, and K directions of the air volume play a significant part in predicting the blast parameters. In this simulation, the grid arrangement of I, J, K (18, 22, 72) is considered for case 2 and case 3.

4.2.1   Air Volume Type 1

For case 1, it is simulated at 5486 mm (18 ft.) away from the centre of the charge weight. The result showed that the peak overpressure for this simulation in free field is 494 kPa at 4.62 msec. as shown in in figure 4.1. From the result on blast test (Case 1) conducted by Yan et. al, (2011), the peak incident overpressure is 490 kPa at 4.64 msec. which it is also recorded at 5486 mm (18 ft.) away from centre of explosive. Besides that, table 4.1 show the comparison of the peak overpressure between

numerical simulation and actual test. The result for the peak overpressure in this simulation is quite similar with the actual blast test form the previous researcher; Yan et. Al (2011). Hence, the numerical results on peak incident overpressure for free field is successfully validated by the actual blast test. So it proved that from the remapped 13.61 kg (30 lbs) TNT charge weight, it is able to simulate the peak overpressure for the next two cases which are for case 2 and case 3.

Table 4.1 Peak overpressure between numerical simulation in free field and actual blast test.

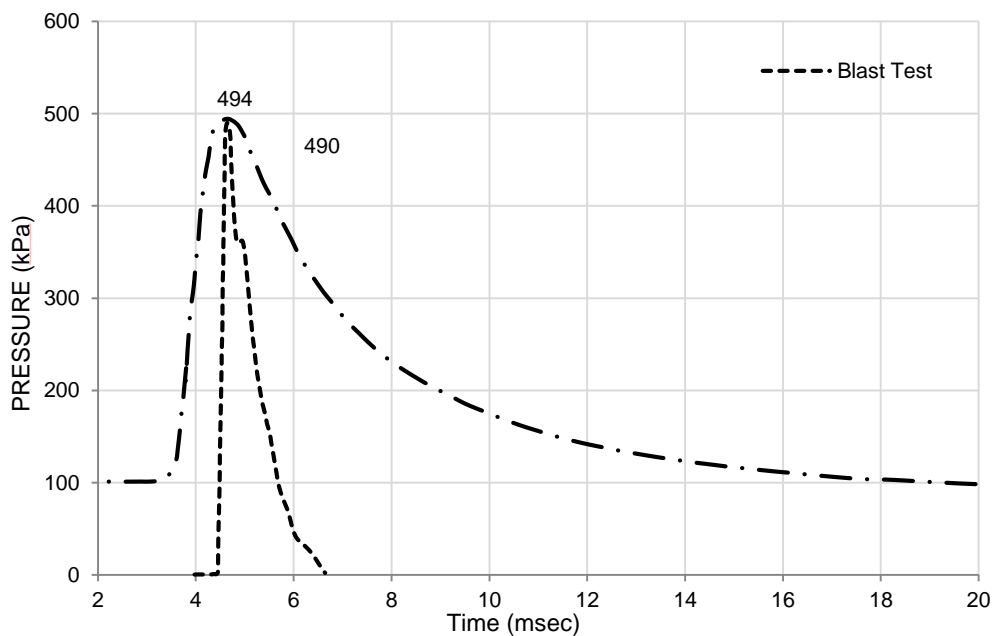|	AUTODYN-Free Field	Blast Test (Yan et. al, 2011)
Pressure (kPa)	494	490
Time (msec.)	4.62	4.64

Figure 4.1 Peak overpressure between numerical simulation in free field and actual blast test

4.2.2 Air Volume Type 2

The results of peak overpressure for 7 gauges without RC wall in case 2 which it located at 1219 mm to 7464 mm away from the charge weight is shown in table 4.2 and figure 4.2. Besides that, figure 4.3 illustrates the blast vector propagations, where it depicts the vector prior to its impact on the simplified vehicle and until the blast vector reached the gauge 7 located at 7464 mm (24.5 ft.) away from the charge weight.

Table 4.2 Results of Peak Pressure without RC Wall as a Barrier (Case 2)

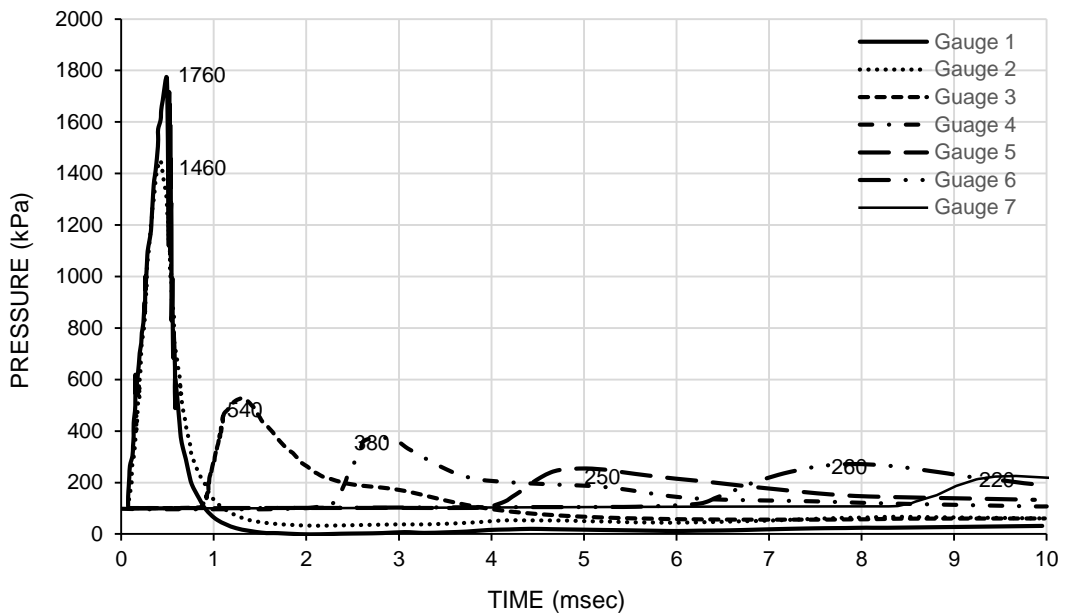| Gauge	Blast Pressure In Case 2 Without RC Wall (kPa)
1	1760
2	1450
3	540
4	380
5	250
6	260
7	220

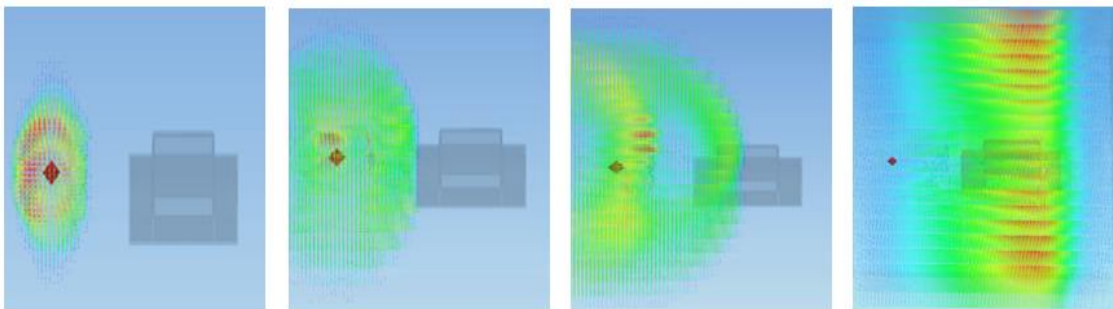Figure 4.2 Pressure Profile Without RC Wall

Figure 4.3 Blast vectors propagation until reached pressure gauge at 7464 mm.

For the overall graph pattern, the result for case 2 shows a decreasing value of blast pressure with increasing value of time and distance.

4.2.3 Air Volume Type 3

The results of peak overpressure for 7 gauges with RC wall in case 3 which it located at 1219 mm to 7464 mm away from the charge weight is shown in table 4.3 and figure 4.3. Besides that, figure 4.4 illustrates the blast vector propagations, where it depicts the vector prior to its impact on the wall, the vector nearly approaches the simplified vehicle and until the blast vector reached the gauge 7 located at 7464 mm (24.5 ft.) away from the charge weight.

Table 4.3 Results of Peak Pressure without RC Wall as a Barrier (Case 3)

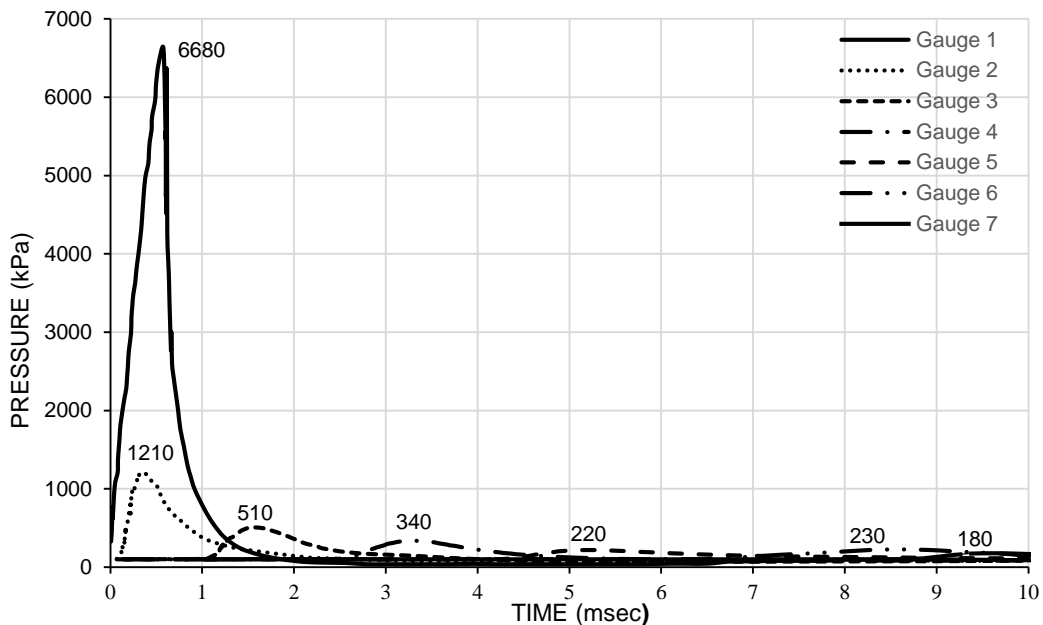| Gauge	Blast Pressure In Case 3 With RC Wall (kPa)
1	6680
2	1210
3	510
4	340
5	220
6	230
7	180

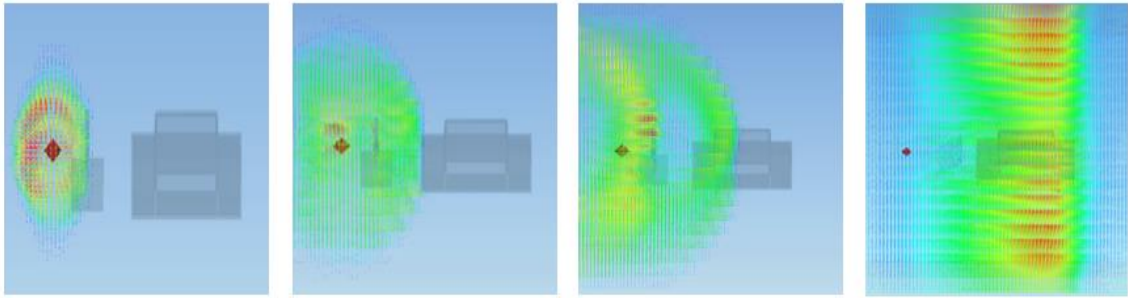Figure 4.4 Pressure Profile With RC Wall

Case 3:

Figure 4.5 Blast vectors propagation until reached pressure gauge at 7464 mm.

Further comparison on blast peak overpressure can be seen in figure 4.5 for the gauge 1 located at 1219 mm away in front of the charge weight, the peak pressure is identical with 1760 kPa at 0.14 msec. and 6680 kPa at 0.19 msec. for case 2 and case 3 respectively. The percentage difference between this two cases is 116.59 %. It shown that the peak overpressure at 1219 mm for case 3 is instantaneously higher compared to case 2. Hence, it can be concluded that with the obstruction of wall nearby the charge weight for gauge 1 in case 3, it shows that the peak overpressure is higher and faster for the gauge compared to the gauge at the same distance with the case without wall as barrier in case 2. It is proved that when the wave encounters a surface, it is reflected and magnified the overpressure.
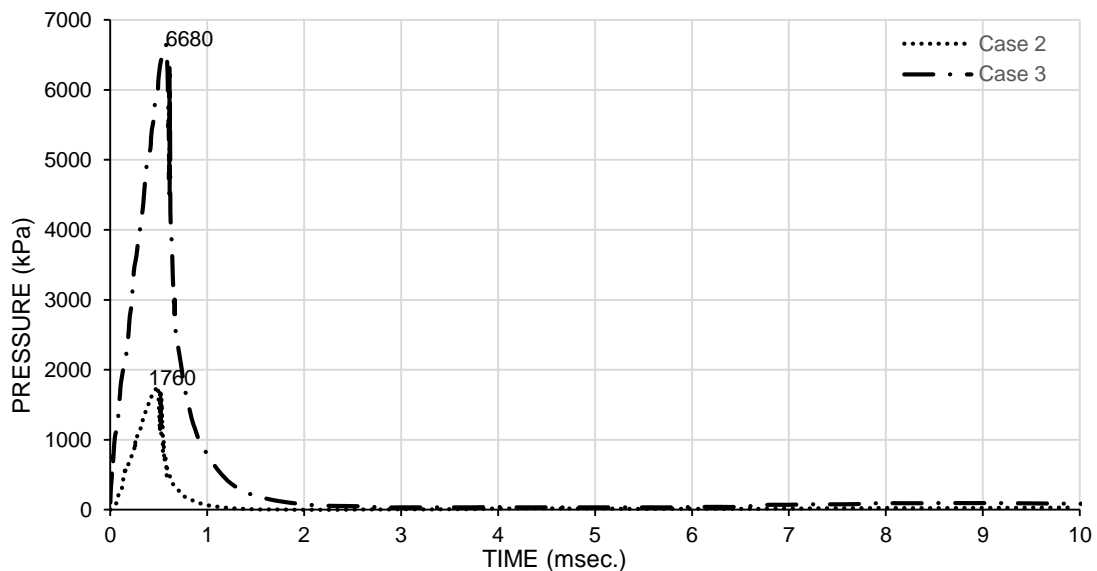

Figure 4.6 Peak overpressure for gauge 1 in case 1 and case 2

Besides that, in figure 4.6 shows the comparison for both cases for gauge 2 located at 1369 mm away from the explosive centre where the location for case 3; with wall as a barrier, this gauge is located exactly behind the wall. Besides, for both cases, these gauges are located at height of 1219 mm from the ground level. The peak overpressure for case 2 is 1450 kPa at 0.24 msec. while for case 3 is 1210 kPa at 0.33 msec. The percentage difference between this two cases is 18.05 %. It shows that overpressure for this gauge in case 3 is lower than in case 2. Therefore, it can be said, when a charge from the blast wave impact the barrier wall, it will diffract around the barrier wall. As a result, the wave is lessened for some distance behind the wall. According to Rouse and Consultants (2012), the area on the backside of the wall is defined as shadow area where the wall affects the blast pressure and cause a pressure reduction. Thus, it can be confirmed from this simulation, the overpressure for the case behind the wall lower than the case without the barrier wall. This is because some percentage of the explosive energy is reflected back and the spreading of the blast pressure behind the barrier wall is changed and the peak overpressure is reduced. Hence, it can provide standoff distances as the peak pressure is reduced which it can protect the vehicles from risky external explosion and can decrease the rate of fatality of the civilians nearby.
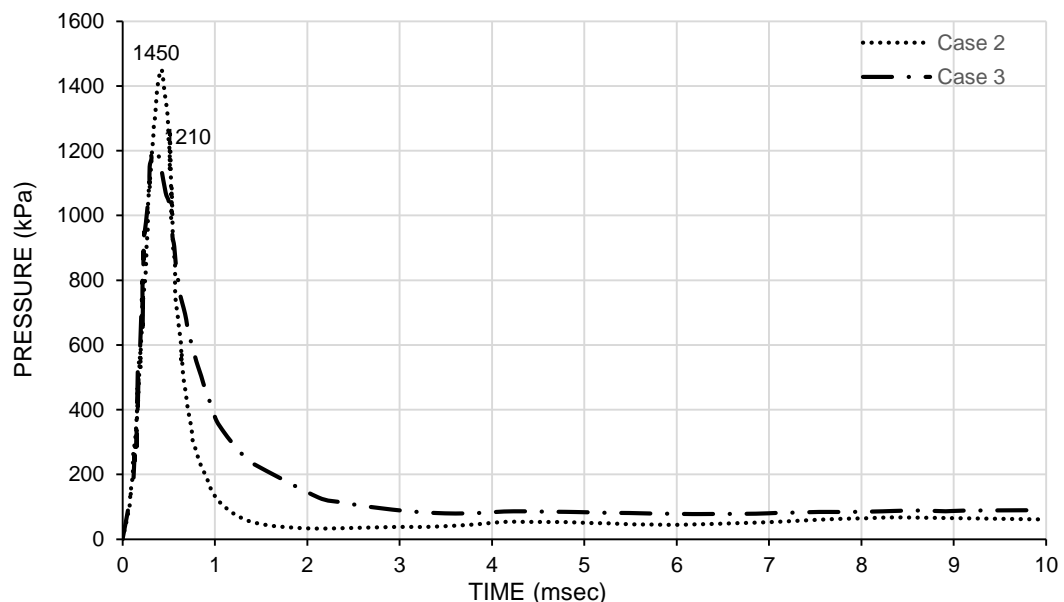

Figure 4.7 Peak overpressure for gauge 2 in case 2 and case 3

In addition, gauge 3 and gauge 8 for both cases are located at 2588 mm away from the centre of the charge weight where both heights are 1219 mm and 609.5 mm respectively from the ground level. The gauge 8 is actually located at the bottom of the gauge 3 for both cases. It shows that the peak overpressure at the bottom is the highest compared to the overpressure at the top for case 2 and case 3. Figure 4.7 and figure 4.8 show that the overpressure- time history for both gauges at the bottom and at top height in case 2 and 3 respectively. The peak overpressure in case 2 for gauge 3 (top) is 540 kPa at 1.28 msec. and for gauge 8 (bottom) is 732 kPa at 1.92 msec. Besides, the peak overpressure in case 3 for gauge 3 (top) and gauge 8 (bottom) is 510 kPa at 1.54 msec. and 595 kPa at 1.56 msec. respectively. According to the experiment conducted by Yan et. al, (2011) in 3 different height of gauges where at the bottom, middle and top, it is found that the peak strain at the bottom of the front face is larger than in the middle height. Normally for case 3 in these wave propagation situation, when there is an obstacle, the blast wave will reach the front face first where it will encounter the surface wall. In this situation, the reflection wave will be produced. Aside from the reflection wave, both rejection wave and transmission wave will be produced when it transmits the waves through the wall and arrived at the back face. Furthermore, in addition of direct wall and its reflection, the reflection wave on the base surface will have vigorous impact on the bottom part of the wall. Thus, it will cause larger deformation at the bottom part of the wall than at the top part when the combination of all these waves occurred. Therefore, the highest peak overpressure that obtained from this numerical simulation at the bottom part compared to the top part is validated for each cases. However, when compared the bottom part for gauge 8 and top part for gauge 3 between case 2 and case 3, it shows that the case 2 has higher peak overpressure for both part. This might happen due to the no reflection occurs at case 2 when there is no barrier wall at this case and the blast wave will propagate hemi-spherically through the air.
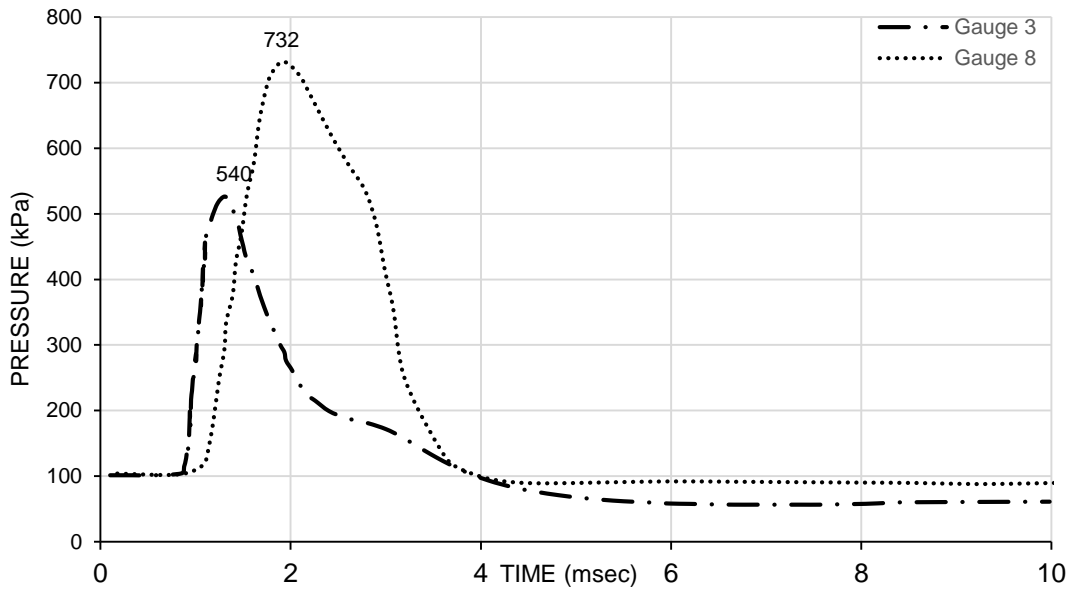
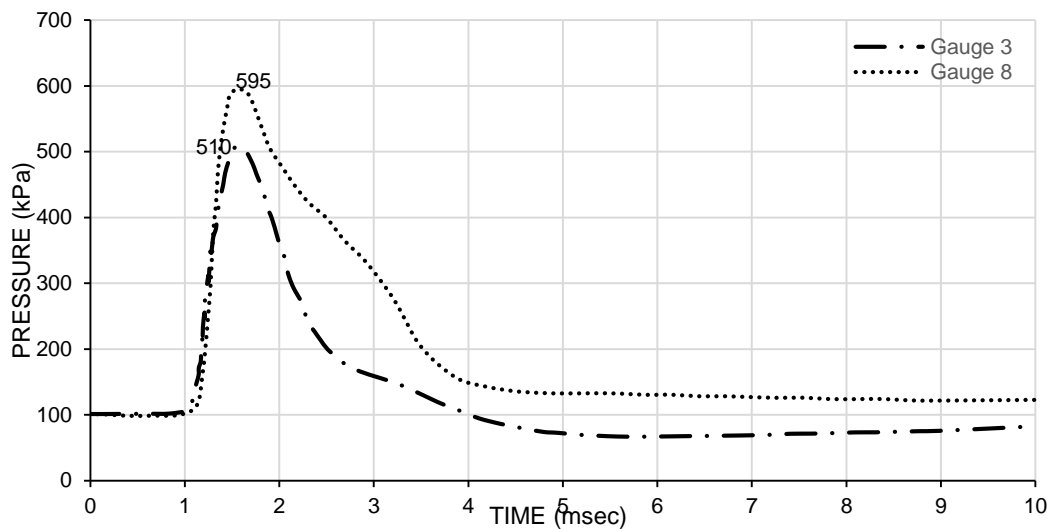Figure 4.8 Peak overpressure for gauge 3 and gauge 8 in case 2

Figure 4.9 Peak overpressure for gauge 3 and gauge 8 in case 2

Moreover, in figure 4.9 shows the comparison for both cases for gauge 3 located at 2588 mm away from the explosive centre. Besides, for both cases, these gauges are located at height of 1219 mm from the ground level. The peak overpressure for case 2 is 540 kPa at 1.28 msec. while for case 3 is 510 kPa at 1.54 msec. The percentage difference between this two cases is 5.71 %. It shows that overpressure for this gauge in case 3 is lower than in case 3. Thus, it can be said that with the present of wall as a barrier, it can decrease the blast pressure and also can delay the time arrival for the blast
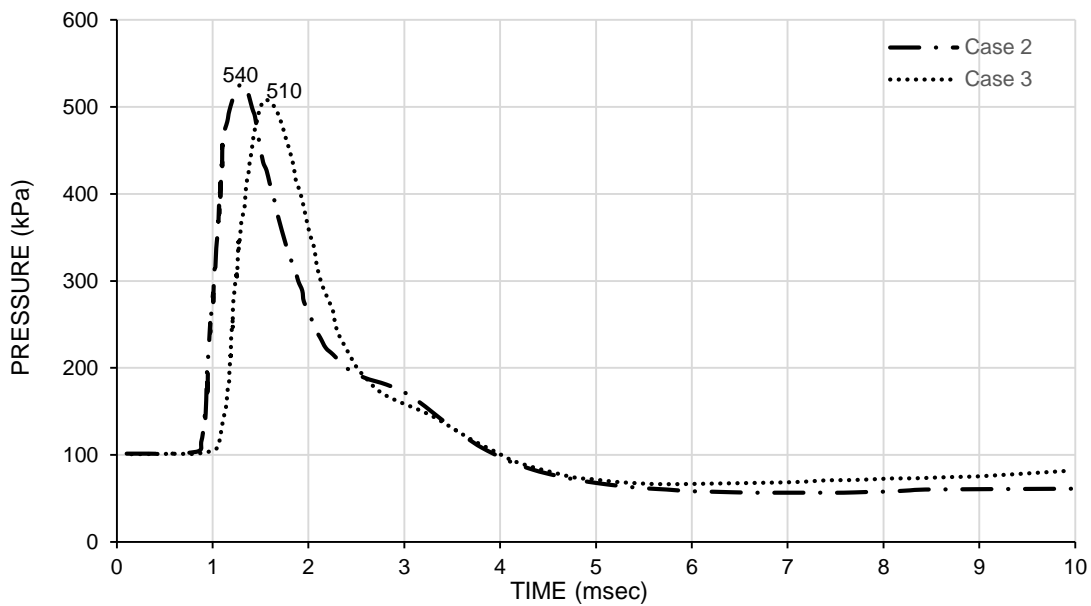
wave.

Figure 4.10 Peak overpressure for gauge 3 in both cases

In addition, for figure 4.10 (a), (b) and (c) show the peak overpressure-time history for gauge 4, gauge 5 and gauge 6 respectively for case 2 and case 3. The location for gauge 4 is 3807 mm away from the centre of the charge weight meanwhile for gauge 5 and gauge 6 are located at 5026 mm and 6245 mm respectively away from the centre of the charge weight. The peak overpressure for gauge 4 in case 2 is 380 kPa at 2.93 msec. and for case 3 is 340 kPa at 3.18 msec. Besides, for gauge 5 in case 2 is 280 kPa at 5.14 msec. and in case 3 is 220 kPa at 5.19 msec. while for gauge 6 in case 2 is 260 kPa at 7.90 msec. and in case 3 is 230 kPa at 8.44 msec. It can be noticed that the gauges located inside the car for case 2 is higher than the gauges for case 3. Thus, it is proved that with existence of the barrier wall in case 3, it can acts as an obstacle in the direction of the blast wave propagation (Zhou and Hao, 2009). Besides that, it is not only can be as an obstacle to the wave propagation but it can reduce the peak overpressure behind the blast wall and also can delay the time arrival of the blast wave. Thus, it also can minimize the casualty and fatality to civilians especially in the car.
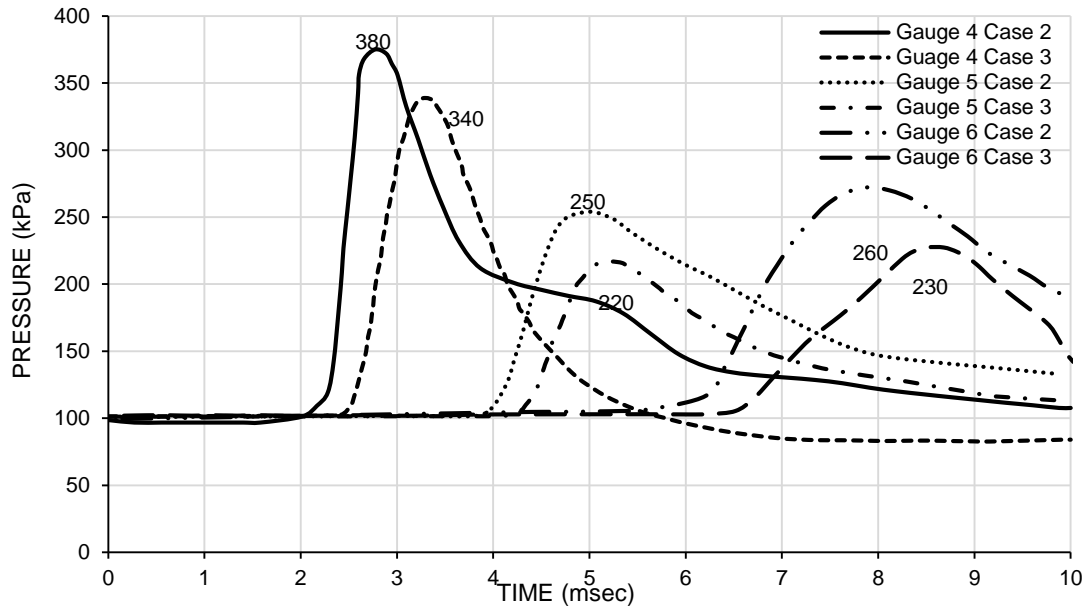
45

Figure 4.11 Peak overpressure for gauge 4, gauge 5 and gauge 6 in case 2 and case 3

From the experiment conducted by Kang, Lehman and Carragee (2012), it reported that the result at the peak overpressure outside a vehicle is approximately 28 times than inside the car which the risk of overpressure injuries is higher when outside a vehicle. For case 2, the peak overpressure for gauge 5 which is inside the vehicle is identical with 250 kPa at 5.14 msec. which is the lower pressure compared to the peak overpressure for the gauges outside the vehicle which are gauge 3, gauge 4, gauge 6 and gauge 7 that identical with 540 MPa at 1.28 msec., 380 kPa at 2.93 msec., 260 kPa at 7.90 msec. and 220 MPa at 7.90 msec. respectively. Figure 4.11 shows that the peak overpressure-time history for these selective gauges in case 2. However, for case 3, the peak overpressure for gauge 5 where it located inside the vehicle is identical with 220 kPa at 5.19 msec. which also the lower blast pressure compared to the peak overpressure for the gauges outside the vehicle which are gauge 3, gauge 4, gauge 6 and gauge 7 that identical with 510 kPa at 1.54 msec., 340 MPa at 3.18 msec., 230 kPa at 8.44 msec. and 180 kPa at 9.62 msec. respectively. Figure 4.12 shows that the peak overpressure for these selective gauges in case 3. Thus, from the result for both cases, it can be revealed that the peak overpressure at inside of the vehicle is lower than the peak overpressure outside the vehicle. Hence, the overall peak overpressure obtained from numerical simulation is proved with experiment conducted by Kang, Lehman and Carragee (2012).
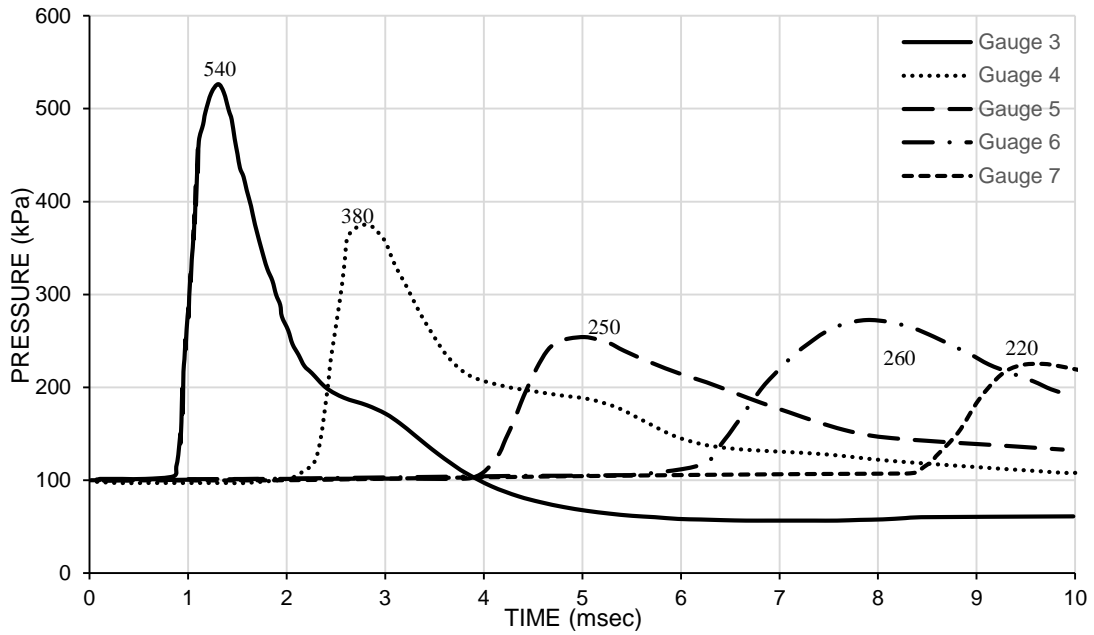
Figure 4.12 Peak overpressure for gauges in case 2
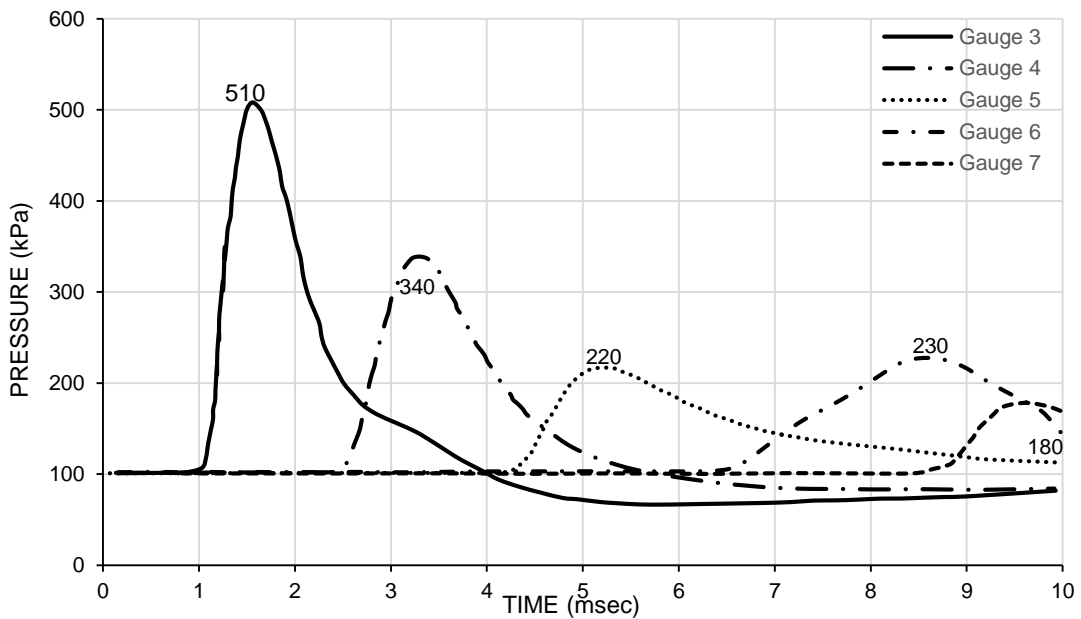
Figure 4.13 Peak overpressure for gauges in case 3

In addition, when the peak overpressure inside of the vehicle is lower than at outside of the vehicle. Hence, the risk of overpressure injuries for the civilians is reduced when inside the vehicle. Generally, the injury pattern in the primary blast occur are varies according to the different impact of pressure. Figure 4.13 below shows that the different blast overpressure for all the gauges inside and outside of the vehicle in case 2 and case 3.

Figure 4.14 Peak overpressure for all gauges in case 2 and case 3

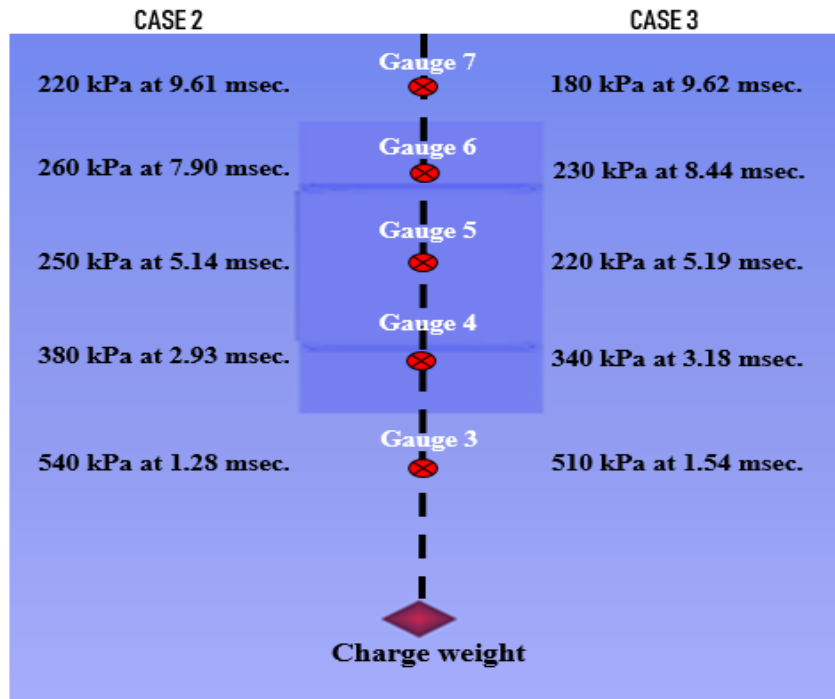Based on the previous researcher by Kang, Lehman and Carragee, (2012) in table 2.2 chapter 2, both of the cases have the same ranges of pressure which is 30 psi to 80 psi which is around 206 kPa to 551 kPa in pressure. If the person inside the vehicle are exposed to an overpressure of 260 kPa for case 2 and 290 kPa for case 3, he may result in the lung injury, pneumothorax, air embolism or intestinal emphysema. Although the gauge 3 for case 2 and case 3 exposed to the highest peak overpressure than the other gauges about 540 kPa and 510 kPa respectively, both of it are in the same pressure range as the gauge inside the vehicle which is this person would likely to experience a similar pattern of injuries in lung injury, pneumothorax, air embolism or intestinal emphysema.

However, based on the previous researcher by Zipf, Kenneth and Cashdollar, (2010) in the table 2.2 chapter 2, if the person inside the vehicle which are for gauge 5 are exposed to an overpressure of 250 kPa for case 2 and 220 kPa for case 3, that person may result in threshold of fatalities. Besides, for case 2 and case 3 of gauge 3, it exposed to the highest peak overpressure than the other four gauges about 540 kPa and 510 kPa respectively. So, the person at this location likely to experience 100 % of fatalities.

4.3 Summary

In this numerical simulation, it initially conducted in 3D free air explosion in 1000 mm x 1000 mm x 5500 mm volume of air for case 1. The result for the peak overpressure is 494 kPa at 4.62 msec. in free field simulation is quite similar with the actual blast test form the previous researcher; Yan et al., (2011) which is 490 kPa at 4.64 msec. So it proved that from the remapped 13.61 kg (30 lbs) TNT charge weight, it is able to simulate the peak overpressure for the next two cases which are for case 2 and case 3. In this simulation, the grid arrangement of I, J, K (18, 22, 72) is considered for case 2 and case 3. Based on the comparison between two cases which are for case 2 and case 3, it can be concluded that the peak overpressure for case 3 is lower than peak overpressure in case 2. Therefore, for overall results show that the blast pressure reduced when there is barrier wall nearby the blast event compared when there is no wall at blast event. For both cases, it shows that the peak overpressure at inside of the vehicle is lower than the peak overpressure outside the vehicle. Hence, the risk of overpressure injuries for the civilians is reduced when inside the vehicle.

CHAPTER 5

CONCLUSION AND RECOMMANDATIONS

5.1   Conclusion

A three-dimensional material model including reinforced concrete model, vehicle model, explosive and air using non-linear finite element analysis software ANSYS- AUTODYN has been performed to predict related parameters of vehicle with and without wall as a barrier under blast load. The comparison of numerical results has been made regarding two different cases which is for case 2 and case 3. According to the result presented in chapter 4, it is clear that the overall result for the peak overpressure of gauge 3, gauge 4, gauge 5, gauge 6 and gauge 7 in case 3 will be reduced with the present of wall compared to the peak blast overpressure in case 2 with no RC wall as barrier. It is found that the barrier walls between an explosion and a vehicle can not only reduce the peak overpressure and impulse on the surface of the vehicle, but also delay the arrival time of the blast wave. It must be noted the effectiveness of a blast barrier in reducing the blast pressure on structures behind the barrier depends not only on the barrier height, distances between the barrier and the vehicle, but also on the width of the barrier wall. Thus, when the pressure is reduced, it will provide standoff distance that can protect the vehicles from extremely explosion and can decrease the rate of fatality.

In addition, overall result for the peak overpressure of gauge 1 in case 3 is higher than peak overpressure for case 2. This is because when the wave encounter the surface of barrier wall, the reflection will occur and it will magnify the overpressure. Thus it will increase the blast overpressure to that surrounding compared to the situation in case 2. This revealed that when an explosion occurs with an obstruction to the propagation blast wave for example to the wall structure, as the blast strikes the wall surface at normal angle of incident, the overpressure is magnified due to blast wave propagation through air suddenly arrested and redirect by the wall surface. Thus for the result, the increased in magnified of the overpressure will occur. Besides, the numerical

result shows that the blast overpressure inside and outside of the vehicle will be reduced about 7 percent of difference when there is present of wall as barrier. Thus, the peak overpressure inside of the car will be lower compared to the peak overpressure outside of the vehicle. However, the gauge 3 and gauge 5 is in the different location and blast pressure result, those are likely in same pattern of injury which is the person at both locations possibly will die. This is because 30 lbs TNT is quite high. So as for recommendation will used the lower TNT weight.

5.2   Recommendation for Future Study

In this research, there are several recommendations were identified which needed to be considered for future investigation in order to provide a more reliable data for better result in this numerical result. The following fields are suggested to expand the present work by:

1. To used different charge weight such as 10 and 20 lbs. to compare the blast pressure parameter.
2. Put series number of RC wall as barrier. The size of the wall used before is smaller than the size of simplified vehicle which is not covered enough the width of the vehicle.
3. The material properties of each element used in the simulation such as concrete and steel reinforcement of the RC wall must be obtained from laboratory work before simulation being conducted to ensure the outputs of analysis are more accurate.
4. Replace the current simplified car with the actual design of the vehicle. So, the dimension of the vehicle more accurate and get more reliable data.

REFERENCES

Alexander, S., George, S., Laurent, T., and Arja, S., 2013. Resistance of Structures to Explosion Effects: Review Report of Testing Methods ERNCIP Thematic Area

Ali, N.M., Mohsin, S.M.S, Seman, M.A. and Jaini, Z.M., 2015. Numerical Prediction of Cantilevered Reinforced Concrete Wall Subjected to Blast Load.

ANSYS. (2017). *Release 17.0.* Canonsburg, PA: ANSYS, Inc.

ANSYS, 1997. Structural nonlinearities, User's guide for revision 5.5. , p.

Draganić, H. and Sigmund, V., 2012. Blast loading on structures. Tehnički vjesnik, 19(3), pp.643–652.

Kang, D.G., Lehman, R.A. and Carragee, E.J., 2012. Wartime spine injuries: Understanding the improvised explosive device and biophysics of blast trauma. Spine Journal, 12(9), pp.849–857. Available at: http://dx.doi.org/10.1016/j.spinee.2011.11.014.

Kontodimos, A., 2017. Lethal Use of Armed Drones and the "War on Terror." , pp.587–632.

Malhotra, A., Carson, D. and McFadden, S., 2017. Blast pressure leakage into buildings and effects on humans. Procedia Engineering, 210, pp.386–392. Available at: https://doi.org/10.1016/j.proeng.2017.11.092.

Marx, J., Portanova, M. and Rabiei, A., 2019. Ballistic Performance of Composite Metal Foam against Large Caliber Threats. Composite Structures, (May), p.111032. Available at: https://linkinghub.elsevier.com/retrieve/pii/S0263822319312607.

Mirgal, P., Tikate, P., Suryawanshi, S. and Tande, S.N., 2014. Architectural and Structural Design for Blast Resistant Buildings. Journal of Civil Engineering and Environmental Technology, 1(3), pp.103–108.

Olarewaju, A.J., Kameswara Rao, N.S.V. and Mannan, M.A., 2010. Response of underground pipes due to blast loads by simulation - an overview. Electronic Journal of Geotechnical Engineering, 15 H, pp.1–22.

Peng, W., 2009. Modeling and simulation of interactions between blast waves and structures for blast wave mitigation. -- …Mechanical (and Materials) Engineering, p.102. Available at: http://digitalcommons.unl.edu/cgi/viewcontent.cgi?article=1004&context=mech engdiss.

Ramasamy, A., Hughes, A., Carter, N. and Kendrew, J., 2013. The effects of explosion on the musculoskeletal system. Trauma, 15(2), pp.128–139.

Remennikov, A., 2007. The state of the art of explosive loads characterisation. , pp.1–25.

Rouse, N. and Consultants, M.W., 2012. The Mitigation Effects of a Barrier Wall on Blast Wave Pressures. International Society of Explosive Engineers, pp.1–8.

Theses, M. and Baumgart, C.M., 2014. The effects of advanced structural materials to mitigate explosive and impact threats Presented to the Faculty of the Graduate School of the In Partial Fulfillment of the Requirements for the Degree.

Thomas, R.J., Steel, K. and Sorensen, A.D., 2018. Reliability analysis of circular reinforced concrete columns subject to sequential vehicular impact and blast loading. Engineering Structures, 168(May), pp.838–851. Available at: https://doi.org/10.1016/j.engstruct.2018.04.099.

Wolf, S.J., Bebarta, V.S., Bonnett, C.J., Pons, P.T., and Cantrill S.V., 2009. Blast injuries. The Lancet, 374(9687), pp.405–415. Available at: http://dx.doi.org/10.1016/S0140-6736(09)60257-9.

Yang, Y. et al., 2013. Shock wave impact simulation of a vehicle occupant using fluid/structure/dynamics interactions. International Journal of Impact Engineering, 52, pp.11–22. Available at: http://dx.doi.org/10.1016/j.ijimpeng.2012.09.002.

Yusof, M.A., Szer, L.W., Nor, N.M., Ismail, A., Yahya, M.A. and Peng, N.C., 2014. Simulation of Annealed Glass Panels Subjected to Air Blast Loading. , 4(8), pp.430–434.

Zhou, X.Q. and Hao, H., 2009. Prediction of airblast loads on structures behind a protective barrier. International Journal of Impact Engineering, 35(5), pp.363–375.

Zipf, R.K., Kenneth, P.E. and Cashdollar, L., 2010. Explosions and Refuge Chambers: Effects of blast pressure on structures and the human body. Available at: https://www.cdc.gov/niosh/docket/archive/pdfs/NIOSH-125/125-ExplosionsandRefugeChambers.pdf.

APPENDIX